Tissue Engineering
© Mary Ann Liebert, Inc.
DOI: 10.1089/ten.TEA.2017.0379

Downloaded by Guangxi University for Nationalities from online.liebertpub.com at 02/17/18. For personal use only.

Tissue Engineering
Cross-linked cholecyst-derived extracellular matrix for abdominal wall repair (DOI: 10.1089/ten.TEA.2017.0379)
This paper has been peer-reviewed and accepted for publication, but has yet to undergo copyediting and proof correction. The final published version may differ from this proof.

Type:

Original Research

Title:

Cross-linked cholecyst-derived extracellular matrix for abdominal wall repair

Authors:

Jeffrey C.Y. Chan[1,2], Krishna Burugapalli[3], Yi-Shiang Huang[2], John L. Kelly[1,2], Abhay Pandit[2]

[1]Department of Plastic, Reconstructive and Hand Surgery, University Hospital Galway, Galway, Ireland

[2] CÚRAM, Centre for Research in Medical Devices, National University of Ireland Galway, Ireland

[3]Biomedical Engineering Theme, Institute for Environment Health and Societies, Brunel University, Uxbridge, Middlesex, UB8 3PH, United Kingdom

Jeffrey Chee Yean Chan, MBBChBAO, MMedSc(Hons), MRCS, FRCS(Plast)

Tel: N/A

Fax: N/A

Email: jeff.chan@me.com

Krishna Burugapalli, BSc, MSc, PhD

Tel: N/A

Fax: N/A

Email: krishna.burugapalli@brunel.ac.uk

Yi-Shiang Huang, BSc, MSc, PhD

Tel: +353 (0) 91 49 5902

Fax: N/A

Email: yi-shiang.huang@nuigalway.ie

John L. Kelly, MB, MD, FRCS, FRCS(Plast)

Tel: N/A

Fax: N/A

Email: N/A

Corresponding author:

Prof Abhay Pandit

Tel: 00353 91 492758

Fax: N/A

Email: abhay.pandit@nuigalway.ie

Downloaded by Guangxi University for Nationalities from online.liebertpub.com at 02/17/18. For personal use only.

Tissue Engineering
Cross-linked cholecyst-derived extracellular matrix for abdominal wall repair (DOI: 10.1089/ten.TEA.2017.0379)

This paper has been peer-reviewed and accepted for publication, but has yet to undergo copyediting and proof correction. The final published version may differ from this proof.

Downloaded by Guangxi University for Nationalities from online.liebertpub.com at 02/17/18. For personal use only.

Tissue Engineering
Cross-linked cholecyst-derived extracellular matrix for abdominal wall repair (DOI: 10.1089/ten.TEA.2017.0379)

This paper has been peer-reviewed and accepted for publication, but has yet to undergo copyediting and proof correction. The final published version may differ from this proof.

Abstract:

Abdominal wall repair frequently utilizes either non-degradable or bio-degradable meshes, which are found to stimulate undesirable biological tissue responses or which possess suboptimal degradation rate. In this study, a biologic mesh prototype made from carbodiimide-cross-linked cholecyst-derived extracellular matrix (EDCxCEM) was compared with small intestinal submucosa (Surgisis®), cross-linked bovine pericardium (Peri-Guard®), and polypropylene (Prolene®) meshes in an *in vivo* rabbit model. The macroscopic appearance and stereological parameters of the meshes were evaluated. Tailoring the degradation of the EDCxCEM mesh prevents untimely degradation, while allowing cellular infiltration and mesh remodelling to take place in a slower but predictable manner. The results suggest that the cross-linked biodegradable cholecyst-derived biologic mesh results in no seroma formation, low adhesion, and moderate stretching of the mesh. In contrast to Surgisis®, Peri-Guard®, and Prolene® meshes, the EDCxCEM mesh showed a statistically significant increase in the volume fraction (V_v) of collagen (from 34% to 52.1%) in the central fibrous tissue region at both day 28 and day 56. The statistically high Length density (L_v), of blood vessels for the EDCxCEM mesh at 28 days was reflected also by the higher cellular activity (high V_v of fibroblast and moderate V_v of nuclei) indicating remodelling of this region in the vicinity of a slowly degrading EDCxCEM mesh. The lack of mesh area stretching/ shrinkage in the EDCxCEM mesh showed that the remodelled tissue was adequate to prevent hernia formation. The stereo-histological assays suggest that the EDCxCEM delayed degradation profile supports host wound healing processes including collagen formation, cellular infiltration, and angiogenesis. The use of cross-linked cholecyst-derived extracellular matrix for abdominal wall repair is promising.

Keywords: carbodiimide crosslinking, cholecyst-derived extracullar matrix, abominal wall repair, rabbit animal model, mesh stretching.

Downloaded by Guangxi University for Nationalities from online.liebertpub.com at 02/17/18. For personal use only.

Tissue Engineering
Cross-linked cholecyst-derived extracellular matrix for abdominal wall repair (DOI: 10.1089/ten.TEA.2017.0379)

This paper has been peer-reviewed and accepted for publication, but has yet to undergo copyediting and proof correction. The final published version may differ from this proof.

Introduction

In abdominal wall hernia, weakness or the absence of the abdominal wall leads to protrusion of intra-abdominal organs through this weakened area – presenting clinically as bulging or swelling in the area. The goal of abdominal wall repair is the restoration of abdominal wall so that it is sufficient to contain abdominal wall organs from herniation during physiological levels of stress. In primary hernia repairs, the recurrence rate of hernia can be as high as 50% (1-5). As a result, it has become a common practice to reinforce the abdominal wall with surgical meshes that at least halved the recurrence rate (1, 4). However, the risk of recurrence must be balanced against the risk of mesh related complications such as infection, seroma, wound dehiscence and enterocutaneous fistula.

Synthetic non-degradable surgical meshes used for abdominal wall reconstruction can stimulate an intense foreign body response, leading to mesh area contraction (6-8). This abnormal tissue reaction is thought to contribute to abdominal wall stiffness, mesh-related complications and chronic pain (9-11). Although there is no hernia recurrence, the implant repair area is contracted and stiff. Strategies such as increasing the pore size of meshes and manufacturing lighter synthetic meshes attempt to overcome this problem (7, 12-16). In some studies, adoption of lighter meshes were associated with a higher recurrence rate of hernias (14, 17-19) and no advantage in reduction of chronic pain (20-23). In the presence of infection or potential contamination, synthetic mesh repair is not recommended as it is associated with a high risk of infection, pain and hernia recurrence (24-26).

Degradable allogenic/xenogenic biologic meshes have been widely used in the last decade to overcome the undesirable effects of synthetic meshes in high risk patients (contamination or potential contamination, high recurrence group) (27-32). Although these meshes alleviate the need for a staged abdominal reconstruction, there is accumulating evidence to suggest that these meshes are associated with stretching of the repaired area and high failure rates (28, 33-35). This phenomena presents clinically as abdominal wall bulging, abdominal wall laxity and hernia recurrence (36, 37).

The phenomena observed with biologic meshes have been attributed to the inherent properties of the material. The presence of aged dermal collagen and elastin

Downloaded by Guangxi University for Nationalities from online.lieberpub.com at 02/17/18. For personal use only.

Tissue Engineering
Cross-linked cholecyst-derived extracellular matrix for abdominal wall repair (DOI: 10.1089/ten.TEA.2017.0379)

This paper has been peer-reviewed and accepted for publication, but has yet to undergo copyediting and proof correction. The final published version may differ from this proof.

fibres in dermal-derived materials is considered prone to stretching (37, 38). In addition, the rapid in vivo degradation of non-crosslinked meshes in the presence of contamination leads to inadequate restoration of the native abdominal tissue in a timely manner. Methods to improve the performance of biologic meshes have been employed, which includes the creation of multi-laminate constructs to increase bulk and mechanical strength, sourcing xenogenic foetal dermal-derived meshes, utilising non-dermal meshes and crosslinking processes to prevent degradation (34-36). Unfortunately, constructing multi-laminate meshes and crosslinking process are associated with seroma formation (39). Cross-linking strategies such as glutaraldehyde render the biomaterial non-degradable.

For optimal abdominal wall regeneration, it is important that a desired biological tissue response is achieved. This includes a controlled degradation rate of the implanted mesh which would allow replacement of the mesh with host tissues with subsequent timely remodelling of the tissues to restore the function of the abdominal wall.

Neither non-degradable synthetic meshes nor rapidly degradable biologic meshes meet these criteria whereas a slowly degrading extracellular matrix (ECM) could fulfill the required needs for abdominal wall repair by prolonging mesh degradation and tissue remodelling. Herein, a prototype of slowly degrading EDC-crosslinked cholecyst-derived extracellular matrix (EDCxCEM) was developed and its performance was compared with commercially available meshes which were small intestinal submucosa (Surgisis®), crosslinked bovine pericardium (Peri-Guard®), and polypropylene mesh (Prolene®) in an *in vivo* rabbit model (40).

1. Materials and methods

1.1. Materials

All reagents unless otherwise stated were purchases from Sigma Ireland, Ltd., Dublin, Ireland. Fresh cholecysts of market weight farm-reared pigs were obtained from the local supplier Sean Duffy Exports Ltd., Gort, Ireland.

Preparation of cross-linked CEM meshes

CEM was isolated and processed according to a method described elsewhere (41). CEM meshes were then subjected to lyophilisation. Lyophilized CEM meshes were

Downloaded by Guangxi University for Nationalities from online.liebertpub.com at 02/17/18. For personal use only.

Tissue Engineering
Cross-linked cholecyst-derived extracellular matrix for abdominal wall repair (DOI: 10.1089/ten.TEA.2017.0379)

This paper has been peer-reviewed and accepted for publication, but has yet to undergo copyediting and proof correction. The final published version may differ from this proof.

dissected to approximately 4cm x6 cm in size to match the hernia defects in the rabbit prior to cross-linking. The substrates were then hydrated in pre-cooled 50mM MES buffer on ice prior to cross-linking. EDC-cross-linked CEM (EDCxCEM) meshes were prepared by the carbodiimide crosslinking method (41). The crosslinking feed concentration was 0.01 mmol EDC/NHS (1-ethyl-3-(3-dimethylamino-propyl) carbodiimide/N-hydroxysuccinimide) per mg of CEM. The molar ratio of EDC:NHS was kept constant at 1:1. The cross-linking proceeded in 50mM MES buffer at pH 5.3 and 37°C with intermittent stirring for 4 hours.

The cross-linked CEM meshes were washed at least five times with distilled water to remove excess cross-linker or byproducts. The EDCxCEM meshes were then used immediately or stored at 4^{o}C and implanted within 48 hours. The samples were sterilised with 0.15% peracetic acid in sterile water for at least five minutes, followed by washing in sterile water. Peracetic acid was reported to be an efficient disinfectant that deactivates not only bacteria but also viral loads (42-46). The meshes were then kept hydrated in a solution of sterile normal saline during surgery. Prolene®, Surgisis® (4-layer) and Peri-Guard® meshes were used as per the manufacturer's instruction.

1.2. Implantation in rabbits

Forty eight male New Zealand White Rabbits (weight 3.0 - 3.5 kg) were used for this study. The animals were acclimatised for at least one week to the local environment before surgery. All procedures were conducted under the approval from the Institutional Animal Ethics Committee of National University of Ireland, Galway and a license was obtained from the Department of Health and Children, Dublin, Ireland as required by the Cruelty of Animals Act (1876). Certificate B (No. B100/3685).

Six rabbits were assigned to each group. Hairs were removed from the anterior abdominal wall with electric hair clippers. The rabbits were anaesthetised using intramuscular Ketamine (35mg/kg) and Xylazine (5mg/kg). The hernia defect was created and repaired. Briefly, a midline incision was performed through the skin and subcutaneous fat. The rectus abdominus muscle was exposed on the left side. Excision of the rectus abdominus muscle was performed unilaterally on the left side including the peritoneal layer. A 4 cm longitudinal length was marked on the mid-portion of the rectus abdominus

Downloaded by Guangxi University for Nationalities from online.liebertpub.com at 02/17/18. For personal use only.

Tissue Engineering
Cross-linked cholecyst-derived extracellular matrix for abdominal wall repair (DOI: 10.1089/ten.TEA.2017.0379)

This paper has been peer-reviewed and accepted for publication, but has yet to undergo copyediting and proof correction. The final published version may differ from this proof.

muscle. Excision was carried out for this longitudinal length (4cm) along the borders of the linea alba and the linea semilunaris (width) (40). The resultant abdominal wall defect (the excised mid-portion of the rectus abdominus muscle of 4cm length) was repaired with a similar sized mesh (like for like, "replacement") using a running 4/0 polypropylene suture (tension-free inlay bridging technique). Each rabbit was randomised to receive either a polypropylene mesh (Prolene®, Ethicon Endo-Surgical Inc.), 4-layer small intestinal submucosa graft (Surgisis®, Cook Medical Inc., IN, USA), glutaraldehyde-crosslinked bovine pericardium (Peri-Guard®, Synovis Surgical Innovations) or EDCxCEM. Each rabbit was given a standard dose of prophylactic antibiotic subcutaneous enrofloxacin (5mg/kg) and subcutaneous analgesia butorphanol (0.25-0.4mg/kg) for 48 hours post surgery. The rabbits were maintained in a controlled environment in cages until sacrifice. All rabbits were observed regularly for wound complications including infection, bleeding, seroma and dehiscence. The time periods for the study were 28 days and 56 days.

In the first week post-surgery, the presence of seroma at the mesh site was examined daily, followed by weekly observation from the second week onwards. Examination for possible occurence of abdominal wall hernia was performed weekly until euthanasia.

At 28 days and 56 days, the rabbits were euthanised with intravenous injection of 2 mL sodium pentobarbital (Dolethal®) under anaesthesia. The anterior abdominal wall tissues were removed with care to preserve both rectus abdominis muscles and surrounding tissues. Mesh area stretching or contraction was noted, and any adhesion was removed prior to tracing the size of the mesh area with tracing paper. The mesh area was identified by the presence of polypropylene sutures used for securing the mesh at the time of repair and to identify host tissue ingrowth in place of the mesh.The dimension of the implant was measured as previously described (40). Briefly, the mesh borders were traced using tracing paper and photographs were taken as required. The tracings were scanned to digital images and the mesh area dimensions (width, length and mesh area) were determined using image analysis software (ImageJ v1.43, National Institutes of Health, USA). The percentage contraction/stretching of the area, width or length of the implant area were evaluated with the following formula:

Downloaded by Guangxi University for Nationalities from online.liebertpub.com at 02/17/18. For personal use only.

Tissue Engineering
Cross-linked cholecyst-derived extracellular matrix for abdominal wall repair (DOI: 10.1089/ten.TEA.2017.0379)

This paper has been peer-reviewed and accepted for publication, but has yet to undergo copyediting and proof correction. The final published version may differ from this proof.

Percentage change=[(Implant left side)−(Control right side)]/(Control right side)×100%

The presence of intra-abdominal adhesions were documented and scored using the Surgical Membrane Study Group (1992) scoring system (Figure S1) (47). The mesh areas were then dissected and preserved in 4% neutral buffered formalin.

1.3. Tissue processing and histology analysis

Formalin fixed tissues were dehydrated through a series of graded ethyl alcohol solutions (50, 75, 95 and 100%), cleared with xylene and embedded in paraffin using an automatic tissue processor (Leica ASP 300, Leica Microsystems, Nussloch, Germany). 5 μm thick paraffin sections were stained with Masson's trichrome stain. The stained sections were observed under light microscope and digital images captured for qualitative histomorphology and quantitative stereological analysis (BX51 microscope, DP-70 digital camera, Olympus Europe, Hamburg, Germany)

1.4. Quantitative stereological analysis

The stereological methods used for the quantitative analysis of tissue response and degradation parameters were conducted as previously reported by Garcia et al (48). Briefly, the stereological approach is based on isotropic sampling. Since the abdominal wall is an anisotropic layered structure, it is stratified and requires the use of a vertical uniform random sampling method to obtain isotropy in the vertical sections. At least six non-overlapping random fields of view per section per stereological parameter, six sections per mesh, and six meshes per group per time point were used for adequate sampling. The probes/ test systems (counting grids/cycloids) provided by an image analysis software (ImageJ, National Institutes of Health, USA) were used to enable point counts for stereological estimations.

The mesh site was divided into two regions, namely, the mesh region and the fibrous tissue region surrounding the mesh (Figure S1a). Each region was subdivided into the central area and the peripheral area of the mesh/fibrous tissue regions (Figure S1b). Stereological volume fraction (V_v) estimations of nuclei, fibroblasts and native host collagen and/or residual mesh (mesh collagen or polypropylene fibres) were used to

Downloaded by Guangxi University for Nationalities from online.liebertpub.com at 02/17/18. For personal use only.

Tissue Engineering
Cross-linked cholecyst-derived extracellular matrix for abdominal wall repair (DOI: 10.1089/ten.TEA.2017.0379)

This paper has been peer-reviewed and accepted for publication, but has yet to undergo copyediting and proof correction. The final published version may differ from this proof.

evaluate the tissue composition of each area. Length density (L_v), surface density (S_v) and radius of diffusion (R_{diff}) estimations were used to evaluate the distribution of blood vessels in each area.

1.5. Statistical analysis

Statistical analyses were carried out using statistical software InStat® (GraphPad Software Inc., USA). Statistical differences between groups were analysed by one way analysis of variance (ANOVA). Tukey's honestly significant difference test was used for post hoc evaluation for differences between groups. When the dataset did not satisfy the criteria for parametric tests, Kruskal-Wallis test was used with Dunn's multiple comparisons between groups. A *p* value of <0.05 was considered to be statistically significant. All data represented was expressed as mean ± standard deviation (SD).

2. Results

2.1. Macroscopic tissue explants examination

Figure 1 summarizes the appearance of the meshes after abdominal wall repair surgery at 28 days and 56 days. No infection, skin irritation, ulceration, wound dehiscence; bleeding/ haematoma or development of hernia was observed for all groups. All animals resumed normal activity within 12 to 24 hours after surgery.

Examination of the explanted abdominal wall revealed that all Prolene® meshes and Peri-Guard® meshes remained macroscopically intact until day 56. The degradable meshes (EDCxCEM and Surgisis®) showed different degrees of *in vivo* degradation at day 28 and day 56. Macroscopically, both EDCxCEM and Surgisis® meshes were visible at 28 days. Striking blood vessels and host connective tissue were observed to infiltrate the meshes from the mesh margin/edge of the defect interface. Compared to EDCxCEM, however, Surgisis® showed a more advanced stage of degradation at both 28 days and 56 days. By 56 days, none of the original Surgisis® meshes were observed by macroscopic examination and they had been infiltrated by host tissue, at least on the peritoneal surface of the meshes. In contrast, parts of the EDCxCEM meshes were visible at day 56 and showed evidence of degradation and host tissue replacement. There was no mesh area stretching

observed for both the EDCxCEM and Surgisis® meshes at day 28. By day 56, stretching of the Surgisis® meshes was evident. A much lesser degree of stretching of EDCxCEM meshes was observed.

Figure 2 shows seroma formation for both the Surgisis® and Peri-Guard® meshes during post-operative examinations. 75% of Peri-Guard® meshes showed evidence of seroma formation, typically within the first three days after surgery. In contrast to Peri-Guard® meshes, seroma formation in the Surgisis® group was delayed and typically detected clinically at least after three days post-surgery. There was no seroma observed in the Prolene® and EDCxCEM groups.

Figure 3 shows adhesions which were evaluated upon euthanasia. All Surgisis® meshes were free of adhesion at both day 28 and day 56. At day 28, the EDCxCEM and Peri-Guard® meshes were free of adhesions. At day 56, adhesions were confined to the suture lines at the mesh-host tissue interface in one rabbit from the EDCxCEM group and two rabbits from the Peri-Guard® group. There was no noticeable complication (such as bowel dilatation or obstruction) from these adhesions. Adhesions complicated 50% of Prolene® meshes at both 28 days and 56 days. These adhesions involved the mesh areas. The area of the mesh involved varied from 30% to 70%. Again, no noticable complications was found due to these adhesions.

2.2. Changes in mesh dimensions

The change of width, length, and total area of the meshes is demonstrated in Figure 4. Surgisis® showed a statistically significant percentage change in mesh width from 5% at day 28 to 30% at day 56. In contrast to Surgisis®, the EDCxCEM mesh did not show a statistically significant percentage change in mesh width (from 2.4% at day 28 to 6.6% at day 56). The Peri-Guard® and Prolene® meshes contracted significantly by day 56 (16.3% and 19.9%, respectively).

As for the change in mesh length, all meshes showed an increase of between 4-10% at day 56. Since the change in length was compared against the initial excision length, some of this increase is likely due to the growth of the animals. No statistically significant difference was observed between groups.

Downloaded by Guangxi University for Nationalities from online.liebertpub.com at 02/17/18. For personal use only.

Tissue Engineering
Cross-linked cholecyst-derived extracellular matrix for abdominal wall repair (DOI: 10.1089/ten.TEA.2017.0379)
This paper has been peer-reviewed and accepted for publication, but has yet to undergo copyediting and proof correction. The final published version may differ from this proof.

Downloaded by Guangxi University for Nationalities from online.liebertpub.com at 02/17/18. For personal use only.

Tissue Engineering
Cross-linked cholecyst-derived extracellular matrix for abdominal wall repair (DOI: 10.1089/ten.TEA.2017.0379)

This paper has been peer-reviewed and accepted for publication, but has yet to undergo copyediting and proof correction. The final published version may differ from this proof.

The pattern of change in mesh area broadly follows the trend in the change of width. Surgisis® showed the most significant percentage change in mesh area. The increase of 5% in area was not significant when compared to other groups at day 28. However, Surgisis® underwent statistically significant stretching between day 28 and day 56, resulting in 48% stretch in area by day 56. Changes to Surgisis® mesh area was significantly difference when compared with all other groups at day 56. The EDCxCEM mesh showed no statistically significant change in mesh area over time (from 3% at day 28 to 12% at day 56). Both the Peri-Guard® (8% to 12%) and Prolene® (12% to 18%) meshes showed increasing mesh area contraction from day 28 to day 56 which were statistically significantly different compared to the Surgisis® and EDCxCEM meshes.

2.3. Descriptive histological analysis

Underneath the cutaneous tissue, all meshes showed fibrous connective tissues directly overlying the meshes. On the underside, a thin layer of neo-peritoneum was evident. Where there were adhesions, the neo-peritoneum was continuous to the adherent tissues. The regions of interest are the mesh region and the fibrous tissue region surrounding the meshes . Each region was subdivided into a central area and a periphery area in relation to the position of the meshes (Figure S1). Figure 5 shows the histology sections of different meshes.

2.3.1. Prolene® (polypropylene)

Histologically, the central area of the mesh region showed multiple circular- or oval-shaped void spaces representing multiple polypropylene filament fibres. Connective tissue surrounded the areas between the filaments. These connective tissues were rich in collagen, fibroblasts and occasional blood vessels. The collagen fibres were arranged in a disorganized manner and encircled polypropylene filaments where they were present. Some collagen bundles appeared more mature (denser and thicker) than other areas (looser and sparse). Inflammatory cells approximately one to five layers thick were intimately related to the polypropylene filaments. There were fibroblasts and sparse inflammatory cells within the connective tissues, away from the polypropylene filaments.

Downloaded by Guangxi University for Nationalities from online.liebertpub.com at 02/17/18. For personal use only.

Tissue Engineering
Cross-linked cholecyst-derived extracellular matrix for abdominal wall repair (DOI: 10.1089/ten.TEA.2017.0379)

This paper has been peer-reviewed and accepted for publication, but has yet to undergo copyediting and proof correction. The final published version may differ from this proof.

There were no apparent difference between the central or peripheral area of the mesh regions between 28 days and 56 days.

In the fibrous tissue region, the tissue was composed of collagen rich connective tissues. Fibroblasts, inflammatory cells and blood vessels were frequently observed in this region. In contrast to the disorganized arrangement in the mesh region, the collagen fibres in this region were more organized and orientated roughly parallel to the long axis of the musculature/surface of the mesh. This fibrous tissue area appeared to be more mature, denser and less cellular at day 56 compared to day 28. There were no difference between the fibrous tissue areas whether they were related to the centre or the periphery of the meshes.

2.3.2. Peri-Guard® (bovine pericardium)

The collagen bundles of bovine pericardia were parallel and compact. The collagen structure in the centre of the Peri-Guard® meshes were intact with no sign of degradation or host cell infiltration. In the mesh region, there was no discernible difference between the appearance of the centre and the periphery areas.

Inflammatory cells (lymphocyte and macrophages) surrounded the surface (five to ten layer thick) and were seen penetrating the surface of the densely packed collagen bundles at the interface between mesh and fibrous tissue regions. Foreign body giant cells were occasionally observed at this interface. There was mild surface degradation of the mesh – evident by short segments of collagen bundles separating away from the main mesh with host cells in between. In the fibrous tissue region, further from the mesh surface, connective tissues with organized collagen, fibroblast, blood vessels and few inflammatory cells were observed. These fibrous tissue areas matured from 28 days to 56 days. A thin neo-peritoneum layer was evident on the underside with a similar inflammatory cellular area at the interface

2.3.3. Surgisis® (small intestinal submucosa)

The collagen bundles of small intestinal submucosa meshes were roughly parallel with occasional curling. A multi-laminated appearance was evident especially in the intact central mesh core region. At 28 days, Surgisis® collagen fibres at the mesh region were

Downloaded by Guangxi University for Nationalities from online.liebertpub.com at 02/17/18. For personal use only.

Tissue Engineering
Cross-linked cholecyst-derived extracellular matrix for abdominal wall repair (DOI: 10.1089/ten.TEA.2017.0379)

This paper has been peer-reviewed and accepted for publication, but has yet to undergo copyediting and proof correction. The final published version may differ from this proof.

intact and acellular, with inflammatory cells infiltrating to approximately 30% to 50% of the thickness of the mesh from the surface. This was observed both at the central and the peripheral of the mesh areas, but more often observed in the central area. The inflammatory cells seen to penetrate the meshes from their surface were dense and composed of lymphocyte and macrophages. Foreign body giant cells were frequently seen with degraded collagen material within the cell bodies. There was some new collagen deposition and fibroblasts at this level.

By 56 days, a large proportions of the mesh had been degraded, leaving behind a thinner region of residual mesh collagen and they were fully infiltrated by host inflammatory cells. By this time, the inflammatory cells were less dense but occupy a larger area. The degraded meshes were replaced by host connective tissues.

In the fibrous tissue region, a dense inflammatory cells layer (ten to twenty layers) was observed at 28 days. These inflammatory cells surrounded and infiltrated the mesh surface layer by layer. By 56 days, this process of degradation was less intense. Connective tissues with a less dense inflammatory cells layers replaced this region previously occupied by mesh collagen bundles.

2.3.4. EDCxCEM (crosslinked CEM)

At 28 days, inflammatory cells were observed to penetrate the surface of the EDCxCEM mesh, approximately 20% of its thickness. The layer of inflammatory cells was much less dense than those seen with Peri-Guard® or Surgisis® meshes. By 56 days, intact collagen bundles within the central mesh region were still present with progression of the host inflammatory cells towards the core of the mesh.

On the surface of EDCxCEM, the fibrous tissue region, degradation of surface collagen bundles was observed. Lymphocytes and macrophages were seen at this interface region. Foreign body giant cells were also seen, having engulfed collagen fibres which had separated from the mesh. Further away from the interface/fibrous tissue region, organised connective tissue comprised of collagen, blood vessels, and fibroblasts were laid down. Occasional inflammatory cells (lymphocytes and macrophages) were also observed but they were more frequent at the mesh surface. The host collagen fibres became denser and their

orientation was more parallel and organised at day 56 indicating maturation and reorganisation of the host connective tissue.

Downloaded by Guangxi University for Nationalities from online.liebertpub.com at 02/17/18. For personal use only.

Tissue Engineering
Cross-linked cholecyst-derived extracellular matrix for abdominal wall repair (DOI: 10.1089/ten.TEA.2017.0379)

This paper has been peer-reviewed and accepted for publication, but has yet to undergo copyediting and proof correction. The final published version may differ from this proof.

2.4 Quantitative stereological analysis

Figure 6 summarizes quantitation of stereological analysis among the groups. Changes to each parameter for each implant type and implant area (central or peripheral) are described, and any noteworthy observations are discussed.

Volume Fraction of Nuclei: Implant Region

In the central area of the implant region, the Vv of nuclei of the EDCxCEM mesh was not significantly different from the other three implant types at 28 days. By 56 days, the Vv of nuclei for EDCxCEM was maintained at a moderate level (3.2%), significantly higher than Peri-Guard® (0.5%) and significantly lower than Prolene® (8.4%) and Surgisis® (7%).

In the peripheral area of the implant region, there was no statistical difference in V_v of nuclei for each individual implant group over time. However, the V_v of nuclei for Prolene® (4.7%) and EDCxCEM (6.4%) was significantly higher than Peri-Guard® (0.5%) at 28 days. By 56 days, the Vv of nuclei of Prolene® (5.4%), Surgisis® (5.7%) and EDCxCEM (3.7%) were all significantly higher than Peri-Guard® (1.8%).

When the central implant area was compared to the peripheral implant area for each group, only the EDCxCEM group showed a statistically higher V_v of nuclei in the peripheral implant area (6.5%) compared to the central implant area (2.6%) at 28 days. These changes indicated that host cellular infiltration was significantly higher at the implant periphery, compared to the centre area for EDCxCEM. The initial higher Vv of nuclei in the peripheral implant area suggested that the porous EDCXCEM implant facilitated early cellular infiltration at the implant periphery. Although, the Vv of nuclei of Prolene® in the peripheral implant area was high, a statistical difference was not observed when compared to the central implant area (3.1% at 28 days; 8.4% at 56 days). This observation was not seen in Peri-Guard® (a densely packed and highly crosslinked collagen) and Surgisis® (a multi-laminate construct).

Volume Fraction of Nuclei: Fibrous Tissue Region

In the central area of the fibrous tissue region at 28 days, EDCxCEM showed a significantly higher V_v of nuclei (4.4%) when compared to Prolene® (1.2%). By 56 days, the V_v of nuclei

Downloaded by Guangxi University for Nationalities from online.liebertpub.com at 02/17/18. For personal use only.

Tissue Engineering
Cross-linked cholecyst-derived extracellular matrix for abdominal wall repair (DOI: 10.1089/ten.TEA.2017.0379)

This paper has been peer-reviewed and accepted for publication, but has yet to undergo copyediting and proof correction. The final published version may differ from this proof.

of Peri-Guard® has increased significantly (by 3 fold to 7.1%) to match that of Surgisis® (8.9%). In contrast, at 56 days EDCxCEM maintained a similar V_v of nuclei (4.4%) as it was at 28 days, which was statistically higher than Prolene® (0.3%), but statistically lower than Peri-Guard® (7.1%) and Surgisis® (8.9%).

In the peripheral area of the fibrous tissue region, the V_v of nuclei for the Prolene® mesh (1.2%) at 28 days was significantly lower than all other implants. Surgisis® (17.7%) however, showed the highest V_v of nuclei at 28 days. The V_v of nuclei of EDCxCEM (5.7%) was significantly higher than Prolene®, and not statistically different from Peri-Guard® or Surgisis®. By 56 days, the V_v of nuclei for Surgisis® had significantly decreased from 17.7% to 7.9% (by more than half) to the V_v of nuclei similar to that for Peri-Guard® (8.9%). EDCxCEM implants showed a V_v of nuclei of 2.2% at 56 days, while V_v of nuclei for Prolene® was 0.4%. The V_v of nuclei of EDCxCEM (2.2%) was statistically different from Peri-Guard® (8.9%), Surgisis® (7.9%) and Prolene® (0.4%).

Similarly, the findings of V_v of nuclei in the fibrous tissue region demonstrated that the tissue response occurred at a faster pace in the periphery, compared to the central area. The initial higher fraction of nuclei in the periphery for Surgisis®, Peri-Guard® and to a lesser extent for EDCxCEM indicates that host inflammatory cells were brought into the region to degrade these implants. Since four layer Surgisis®, is a degradable scaffold, its rapid degradation profile is thought to cause an increased level of cellular activity, demonstrated by the high nuclei V_v at 28 days. In contrast, Peri-Guard® being a non-degradable scaffold, resulted in a sustained and prolonged host inflammatory cellular response to degrade the foreign implant, and toxicity of glutaraldehyde may have intensified the inflammatory response. Since EDCxCEM is also a degradable scaffold, a similar cellular response to Surgisis® was predicted. However, EDCxCEM implants had a slower degradation profile and without the toxicity of glutaraldehyde, and therefore, a reduced V_v of nuclei were observed.

Volume Fraction of Fibroblast – Implant Region

In the central implant region, Prolene® implants showed statistically the highest V_v of fibroblasts for both 28 and 56 days (7.5% and 11%, respectively), Peri-Guard®, Surgisis® and EDCxCEM all showed similar V_v of fibroblasts at 28 days (1.4%, 1.5% and 2.6%, respectively). The V_v of fibroblasts increased significantly to 5.4% for Surgisis® at 56 days.

Downloaded by Guangxi University for Nationalities from online.liebertpub.com at 02/17/18. For personal use only.

Tissue Engineering
Cross-linked cholecyst-derived extracellular matrix for abdominal wall repair (DOI: 10.1089/ten.TEA.2017.0379)

This paper has been peer-reviewed and accepted for publication, but has yet to undergo copyediting and proof correction. The final published version may differ from this proof.

Although the V_v of fibroblasts for EDCxCEM also increased from 2.6% to 4.7%, this was not statistically significant.

At the periphery of the implant region, the V_v of fibroblasts for Prolene® (9.1%) and of EDCxCEM (10.6%) were statistically higher than Peri-Guard® (4%). The V_v of fibroblasts for Surgisis® was 5.2% at 28 days and remained unchanged (5.8%) at 56 days. By 56 days, V_v of fibroblasts of the EDCxCEM mesh increased and was statistically higher (12.8%), when compared to the Peri-Guard® and Surgisis® groups. In comparison, the V_v of fibroblasts of Peri-Guard® and Prolene® decreased to 1.8% and 6.5%, respectively.

Overall, it was observed that the V_v of fibroblasts broadly parallels the V_v of nuclei in the implant region. This supports the suggestion of continous remodeling of the implant region by host inflammatory cells (represented by V_v of nuclei) which degrade and remove the implants, while host fibroblasts (represented by V_v of fibroblasts) replace the implant area with fibrous connective tissues. The high V_v of fibroblasts with Prolene® was related to the spaces between the polypropylene filaments that allowed rapid connective tissue ingrowth both at the central and peripheral areas. This effect was also observed with EDCxCEM at the peripheral implant area (10.6% at 28 days; 12.8% at 56 days) as EDCxCEM has been shown to be fibroporous. However, in the central implant area, the V_v of fibroblasts for EDCxCEM was not as high as at the peripheral implant area at 56 days (4.7%), as it takes time for the fibroblasts to reach the central implant area.

Volume Fraction of Fibroblast – Fibrous Tissue Region

In the central fibrous tissue region, the V_v of fibroblasts for Peri-Guard®, Surgisis® and EDCxCEM were similar at approximately 18% to 20% at 28 days. The Vv of fibroblasts for EDCxCEM (20.2%) was statistically higher than Prolene® (13.1%) in this period. After 56 days, the Vv of fibroblasts for Peri-Guard® (8.9%), Surgisis® (11.9%) and EDCxCEM (12%) decreased to approximately half their initial level and these changes were statistically significant.

The V_v of fibroblasts in the peripheral fibrous tissue region showed the same pattern as the central fibrous tissue region. Peri-Guard®, Surgisis® and EDCxCEM implants all showed high V_v of fibroblasts of up to 20% at 28 days. 'On day 56, the values decreased significantly for Peri-Guard® (5.7%) and Surgisis® (10.1%). The V_v of fibroblasts in both the central area and the peripheral area of the fibrous tissue region did not resemble the implant region.

Downloaded by Guangxi University for Nationalities from online.liebertpub.com at 02/17/18. For personal use only.

Tissue Engineering
Cross-linked cholecyst-derived extracellular matrix for abdominal wall repair (DOI: 10.1089/ten.TEA.2017.0379)

This paper has been peer-reviewed and accepted for publication, but has yet to undergo copyediting and proof correction. The final published version may differ from this proof.

Fibroblasts showed a high volume fraction early in the healing process (28 days), and their density decreased after 56 days. For Prolene®, this process occurred earlier as evident by the lower V_v of fibroblasts at 28 days.

Volume Fraction of Implant (Implant Collagen/ Mesh)

In the central implant region, the V_v of all implant types remained statistically unchanged from 28 days to 56 days. The non-degradable Peri-Guard® showed a stable V_v of 90% throughout the study period. The V_v of Surgisis® decreased from 50% to 41% but this was not statistically significant. The V_v of EDCxCEM was virtually unchanged from 28 days (31.3%) to 56 days (29.6%). The V_v of the polypropylene fibres of Prolene® mesh was also virtually unchanged from 28 days (33%) to 56 days (30.5%).

At the peripheral implant region, EDCxCEM showed a statistically significant decrease in V_v of implant from 28 days to 56 days (18.5% to 6.8%). There was no significant change for Prolene® (18.4% to 27.9%), Peri-Guard® (81% to 84%) and Surgisis® (45.7% to 27%) over time. Although Surgisis® is a degradable implant and the V_v of Surgisis® showed a decrease, it did not reach statistical significance at 56 days. As expected, the V_v of Peri-Guard® was still very high at 84% at 56 days. Although not statistically significant, the V_v of Prolene® mesh showed a visible increase from 18.4% to 27.9% which may indicate the beginning of the process of host tissue maturation and contraction of fibrous connective tissue between its polypropylene mesh filaments.

When comparing the central implant region with the peripheral implant region, only the EDCxCEM group showed a statistically significant decrease in V_v of implant collagen at 56 days (29.6% to 6.8%). The V_v of implant in the peripheral implant area of EDCxCEM at 56 days (6.8%) was statistically lower than for all the other groups (Prolene® (27.9%), Peri-Guard® (84%) and Surgisis® (27%)).

The V_v of implant collagen/ mesh fibres can be used as an indication of scaffold degradation or changes in the mesh-tissue composite. Implant collagen displayed different morphology compared to native host collagen – implant collagens showed a denser and darker colour, generally acellular and they stood out against the background host tissue morphology.

The central implant region showed less statistically significant changes than the peripheral implant region with V_v of implant collagen/ mesh that evaluates scaffold degradation. In

Downloaded by Guangxi University for Nationalities from online.liebertpub.com at 02/17/18. For personal use only.

Tissue Engineering
Cross-linked cholecyst-derived extracellular matrix for abdominal wall repair (DOI: 10.1089/ten.TEA.2017.0379)

This paper has been peer-reviewed and accepted for publication, but has yet to undergo copyediting and proof correction. The final published version may differ from this proof.

vivo degradation of degradable implants (EDCxCEM and Surgisis®) was observed at the peripheral implant area, represented by their respective reduction in V_v of implant collagen over the study period and when compared to their respective central implant areas. The low V_v of Prolene® and EDCxCEM illustrated the degree of porosity within these scaffold structures. In comparison, the dense collagen bundles arrangement in Peri-Guard® and the layered small intestinal submucosa in Surgisis® explained their overall higher V_v. The increase in V_v of Prolene® suggests contraction of the implant area causing mesh contraction.

Volume Fraction of Native Collagen – Implant Region

In the central implant region, there was a high V_v of native host collagen (24.6%) within Prolene® meshes at 28 days, and 56 days (26.7%). The V_v of native collagen for Surgisis® increased from 3.6% at 28 days to 8% at 56 days and the V_v of native collagen for EDCxCEM increased from 11.5% to 19.4%; however both did not reach statistical significance. As expected, Peri-Guard® showed negligible V_v of native collagen.

In the peripheral implant region, the V_v of native collagen for Prolene® mesh was very high at 40% by 28 days, and this level was maintained at an average of 36% at 56 days. Although the V_v of native collagen for Surgisis® showed an increase (6.9% to 10.8%), the changes were not significant. In contrast, EDCxCEM showed a statistically significant increase in V_v of native collagen from 28 days (14.7%) to 56 days (39%). Again, Peri-Guard® showed negligible native collagen in this region.

When the peripheral implant region was compared to the central implant region, only the EDCxCEM mesh showed a statistically significant increase in V_v of native collagen. At 56 days, the V_v of native collagen in the peripheral implant region of EDCxCEM was 39%, significantly higher when compared to its central implant region (19.4%).

Native host collagen was rapidly laid down within the gaps of the Prolene® mesh. The secretion of native extracellular matrix is produced by host tissue fibroblasts. Therefore, the V_v of host collagen resembled the pattern of V_v of fibroblasts in the implant region. Only the V_v of EDCxCEM showed statistical difference between the peripheral and central regions at 56 days. EDCxCEM encouraged collagen deposition by two mechanisms - its fibroporous nature (similar to Prolene® mesh) and the remodelling of implant area

following scaffold degradation, although this remodelling process is likely slower than Surgisis®.

Volume Fraction of Native Collagen – Fibrous Tissue Region

In the central fibrous tissue region, Prolene® showed statistically the highest V_v of native collagen when compared to other groups at both time points. The V_v of native collagen for Prolene® at 28 days was 64%, and 73% by 56 days. The V_v of native collagen for Peri-Guard®, EDCxCEM and Surgisis® were 59.8% to 46%, 41.4% to 43.2%, and 37.2% to 27.2% at 28 days and 56 days, respectively. At 56 days, the V_v of native collagen for Surgisis® was statistically the lowest compared to other groups.

Again in the peripheral fibrous tissue region, Prolene® (64.2%) showed statistically higher V_v of native collagen at 28 days compared to Peri-Guard® (42.9%), and Surgisis® (24.4%), but not to EDCxCEM (34%). EDCxCEM showed a significant increase in V_v of collagen (from 34% to 52.1%) between 28 days and 56 days. None of the other three groups showed this increase over time. By this time, the V_v of EDCxCEM became higher than both Peri-Guard® (36%) and Surgisis® (24%), and no difference to Prolene® (60%).

It was observed that Prolene® mesh showed the highest volume fraction of native collagen deposition at both time points. This was faster for Prolene® because there was no implant degradation in the vicinity that delayed collagen matrix deposition. For the degradable biological scaffolds, however, collagen deposition had to be balanced with the demands of ongoing implant degradation. In the cases of Surgisis® and EDCxCEM, it appeared depositions of collagen were reduced by the presence of degrading scaffolds.

Surface Density of Blood Vessels: Implant Region

In the central implant region, S_v of blood vessels for Surgisis® (1.43×10^4 $\mu m^2/\mu m^3$) was significantly lower than the other groups at 28 days (Prolene® 18.5×10^4 $\mu m^2/\mu m^3$, PeriGuard® 11.5×10^4 $\mu m^2/\mu m^3$, EDCxCEM 20.5×10^4 $\mu m^2/\mu m^3$). After 56 days, Sv of blood vessels for Surgisis® (21.4×10^4 $\mu m^2/\mu m^3$) had increased significantly to level similar to Prolene® (24.7×10^4 $\mu m^2/\mu m^3$) and EDCxCEM (16.1×10^4 $\mu m^2/\mu m^3$). Peri-Guard® showed a lower S_v of blood vessels (2.9×10^4 $\mu m^2/\mu m^3$) even at 56 days as blood vessels were unable to infiltrate the non-degradable and stiff Peri-Guard.

For the peripheral implant region, the S_v of blood vessels in this region was generally higher than the central area due to their location at the implant margins. This is due to the

Downloaded by Guangxi University for Nationalities from online.liebertpub.com at 02/17/18. For personal use only.

Tissue Engineering
Cross-linked cholecyst-derived extracellular matrix for abdominal wall repair (DOI: 10.1089/ten.TEA.2017.0379)

This paper has been peer-reviewed and accepted for publication, but has yet to undergo copyediting and proof correction. The final published version may differ from this proof.

Downloaded by Guangxi University for Nationalities from online.liebertpub.com at 02/17/18. For personal use only.

Tissue Engineering
Cross-linked cholecyst-derived extracellular matrix for abdominal wall repair (DOI: 10.1089/ten.TEA.2017.0379)

This paper has been peer-reviewed and accepted for publication, but has yet to undergo copyediting and proof correction. The final published version may differ from this proof.

increased surface area in contact with host tissue that permits blood vessel infiltration. The S_v of blood vessels for Prolene® (25.3 x 10^4 $\mu m^2/\mu m^3$) was significantly higher than Surgisis® (4.1 x 10^4 $\mu m^2/\mu m^3$) at 28 days while the S_v of blood vessels for the EDCxCEM mesh was not significantly different when compared to the other groups at 28 days. The porosities of Prolene® mesh and EDCxCEM architecture allowed blood vessels in growth. After 56 days, S_v of blood vessels for Surgisis® (25.3 x 10^4 $\mu m^2/\mu m^3$) increased significantly (to level similar to Prolene® [23.6 x 10^4 $\mu m^2/\mu m^3$] and EDCxCEM [22.7 x 10^4 $\mu m^2/\mu m^3$]), likely due to infiltration by cells and implant degradation at this time point. Since Prolene® is a non-degrading macroporous material (allowing blood vessels within the mesh interstices) and EDCxCEM was designed to be slowly degrading (sustained blood vessels ingrowth as EDCxCEM was still undergoing degradation), the Sv of blood vessels were still high at 56 days. As expected, the Sv of blood vessels for PeriGuard® (5.6 x 10^4 $\mu m^2/\mu m^3$) was statistically the lowest when compared to the other groups at this time point.

Surface Density of Blood Vessels: Fibrous Tissue Region

At 28 days, in the central fibrous tissue region, the S_v of blood vessels of the EDCxCEM mesh (52.4 x 10^4 $\mu m^2/\mu m^3$) was statistically higher than PeriGuard® (24.2 x 10^4 $\mu m^2/\mu m^3$) and Surgisis® (19.5 x 10^4 $\mu m^2/\mu m^3$), but not statistically different when compared to Prolene® (39.6 x 10^4 $\mu m^2/\mu m^3$). Both the EDCxCEM and Prolene® meshes had the highest S_v of blood vessels because they promoted early cellular infiltration and angiogenesis was stimulated at this early stage in the fibrous tissue area. After 56 days, the S_v of blood vessels for all four groups were similar which indicated a continued host response to remodel or degrade the implants (EDCxCEM 34.3 x 10^4 $\mu m^2/\mu m^3$, PeriGuard® 23.7 x 10^4 $\mu m^2/\mu m^3$, Surgisis® 33.4 x 10^4 $\mu m^2/\mu m^3$, and Prolene® 32.1 x 10^4 $\mu m^2/\mu m^3$).

In the peripheral fibrous tissue region, the S_v of blood vessels of EDCxCEM (62.2 x 10^4 $\mu m^2/\mu m^3$) in this region was statistically higher than Prolene® (21.9 x 10^4 $\mu m^2/\mu m^3$), PeriGuard® (17.5 x 10^4 $\mu m^2/\mu m^3$) and Surgisis® (31.6 x 10^4 $\mu m^2/\mu m^3$) at 28 days. By 56 days, the S_v of blood vessels of EDCxCEM (40.5 x 10^4 $\mu m^2/\mu m^3$) has reduced and was no longer statistically higher than PeriGuard® (41.2 x 10^4 $\mu m^2/\mu m^3$) and Surgisis® (37.1 x 10^4 $\mu m^2/\mu m^3$). The S_v of blood vessels for Peri-Guard® significantly increased from 28 to 56 days, but there was no difference over time for the other groups. Prolene® showed the lowest overall S_v at its 56 days time point (18.7 x 10^4 $\mu m^2/\mu m^3$) when compared to other

Downloaded by Guangxi University for Nationalities from online.liebertpub.com at 02/17/18. For personal use only.

Tissue Engineering
Cross-linked cholecyst-derived extracellular matrix for abdominal wall repair (DOI: 10.1089/ten.TEA.2017.0379)

This paper has been peer-reviewed and accepted for publication, but has yet to undergo copyediting and proof correction. The final published version may differ from this proof.

groups which indicate completion of tissue remodeling and maturation of the peripheral fibrous tissue region of Prolene®, while this process was still ongoing for the other implants.

Length Density of Blood Vessels: Implant Region

In the central implant region, Prolene® (5.2 x 10^4 µm/µm^3), Peri-Guard® (3.6 x 10^4 µm/µm^3) and EDCxCEM (5.3 x 10^4 µm/µm^3) all showed high L_v of blood vessels, while the L_v of blood vessels for Surgisis® (0.31 x 10^4 µm/µm^3) was statistically the lowest at 28 days time point. The presence of blood vessels within bovine pericardium could be explained by host vasculature present on the surface/edge of Peri-Guard® (3.6 x 10^4 µm/µm^3) as inflammatory cells attempts to infiltrate the collagen structure. After 56 days, the L_v of blood vessels for Surgisis® increased significantly (5.2 x 10^4 µm/µm^3) to L_v similar to Prolene® (4.9 x 10^4 µm/µm^3) and EDCxCEM (5.1 x 10^4 µm/µm^3).This can be explained by cellular infiltration into Surgisis® and progressive degraded at this stage. The L_v of blood vessels for Peri-Guard® at 56 days (1.2 x 10^4 µm/µm^3) was statistically lower when compared to Prolene®, Surgisis® and EDCxCEM. The high initial length density of blood vessels seen with Prolene® and EDCxCEM could be attributed to their porous nature.

In the peripheral implant area, L_v of vessels in this region showed the same pattern as the central implant region. There was a statistically significant increase in L_v of blood vessels for Surgisis® from 28 days (1.03 x 10^4 µm/µm^3) to 56 days (6.4 x 10^4 µm/µm^3). There was no statistical difference when comparing the L_v of blood vessels between the different implant groups at 56 days

Overall, both Prolene® and EDCxCEM showed a uniform L_v of blood vessels for both the central and peripheral implant areas at 28 and 56 days (ranging between 4.7 x 10^4 µm/µm^3 to 5.5 x 10^4 µm/µm^3. In contrast, Peri-Guard® showed a decrease in the L_v of blood vessels from 28 to 56 days for both the central (3.6 x 10^4 µm/µm^3 to 1.2 x 10^4 µm/µm^3) and peripheral implant (4.6 x 10^4 µm/µm^3 to 2.1 x 10^4 µm/µm^3) areas. Surgisis® showed increase in the L_v of blood vessels from 28 to 56 days for both the central (0.31 x 10^4 µm/µm^3 to 5.2 x 10^4 µm/µm^3) and peripheral implant (1.02 x 10^4 µm/µm^3 to 6.4 x 10^4 µm/µm^3) areas.

Downloaded by Guangxi University for Nationalities from online.liebertpub.com at 02/17/18. For personal use only.

Tissue Engineering
Cross-linked cholecyst-derived extracellular matrix for abdominal wall repair (DOI: 10.1089/ten.TEA.2017.0379)

This paper has been peer-reviewed and accepted for publication, but has yet to undergo copyediting and proof correction. The final published version may differ from this proof.

Length Density of Blood Vessels: Fibrous Tissue Region

The L_v of blood vessels in the central fibrous tissue region of EDCxCEM (13.5 x 10^4 µm/µm^3) was statistically higher than PeriGuard® (7.3 x 10^4 µm/µm^3) and Surgisis® (5.4 x 10^4 µm/µm^3) and not significantly different from Prolene® (8.8 x 10^4 µm/µm^3). The was reflected also by the higher cellular activity (high V_v of fibroblast and moderate Vv of nuclei) indicating remodeling of this region in the viscinity of a slowly degrading EDCxCEM implant. There was no statistical difference in the L_v of blood vessels at 56 days between the four groups (Prolene® 7.0 x 10^4 µm/µm^3, Peri-Guard® 7.8 x 10^4 µm/µm^3, Surgisis® 8.2 x 10^4 µm/µm^3 and EDCxCEM 8.2 x 10^4 µm/µm^3).

The L_v of blood vessels in the peripheral fibrous tissue area were similar to the pattern seen at the central fibrous tissue area. The L_v of blood vessels of EDCxCEM (18.8 x 10^4 µm/µm^3) was statistically higher than Prolene® (5.1 x 10^4 µm/µm^3), Peri-Guard® (4.5 x 10^4 µm/µm^3) and Surgisis® (8.04 x 10^4 µm/µm^3) at 28 days. However, there was a statistically significant increase of L_v of blood vessels for Peri-Guard® from 28 (4.5 x 10^4 µm/µm^3) to 56 days (11.0 x 10^4 µm/µm^3) which may be attributed to the continuing angiogenesis to support inflammatory cells to degrade the densely crosslinked pericardium. There was an increase in L_v of blood vessels for Surgisis® from 28 (8.04 x 10^4 µm/µm^3) to 56 days (10.7 x 10^4 µm/µm^3) but this increase was not statistically significant. In comparison, by 56 days, the L_v of blood vessels of Prolene® implants (5.07 x 10^4 µm/µm^3) was statistically the lowest, indicating maturation of its fibrous tissue area. Even though there was a decrease in L_v of blood vessels for the peripheral fibrous tissue area at 56 days for EDCxCEM (12.7 x 10^4 µm/µm^3), indicating the early phase of host tissue maturation in this region, this decrease was not statistically significant.

Radius of diffusion

As expected the radius of diffusion was the lowest in the peripheral fibrous tissue region, followed by central fibrous tissue region. Since blood vessels ingrowth occured from the periphery, it was expected that the central implant area would have delayed vessels ingrowth compared to the peripheral areas. Peri-Guard® and Surgisis® had the highest radius of diffusion at 28 days, and can be explained by their dense architecture or layering that prevented capillary ingrowth. At 56 days, the radius of diffusion for Surgisis® improved

to the levels similar to Prolene® and EDCxCEM. This can be attributed to the degradation of Surgisis® and hence, allowing blood vessels to infiltrate more readily.

Downloaded by Guangxi University for Nationalities from online.liebertpub.com at 02/17/18. For personal use only.

Tissue Engineering
Cross-linked cholecyst-derived extracellular matrix for abdominal wall repair (DOI: 10.1089/ten.TEA.2017.0379)

This paper has been peer-reviewed and accepted for publication, but has yet to undergo copyediting and proof correction. The final published version may differ from this proof.

3. Discussion

Seroma and adhesion formation remained a complication common to non-degradable meshes, whether they were synthetic or biologic in nature. We found that seroma complicated 75% of Peri-Guard® meshes which typically occured within the first three days post-surgery (Figure 2c). Interestingly, all Surgisis® meshes were found to have seroma at 3 days post-surgery. The Peri-Guard® mesh has a naturally thick and dense collagenous matrix that prevented large amounts of fluid from permeating through its layer immediately after surgery. In contrast, although each layer of Surgisis® is thin, Surgisis® is designed as a laminated construct. Once fluid entered these layers (within the initial three days) and coupled with the inflammatory process, trapped fluid within these layers had difficulty escaping (Figure 2a). In a small clinical study comparing abdominal wall closure following open abdominal aortic aneurysm repair with primary closure versus augmentation with Peri-Guard® meshes, seroma occurred in 10% of patients repaired with Peri-Guard® meshes (49). However, the authors had anticipated this and made multiple small incisions in the mesh during surgery and inserted drains to prevent seroma formation. The problem with the design of multi-layered Surgisis® was highlighted by Gupta and co-authors who reported a rate of seroma formation as high as 91%. Explanted Surgisis® meshes revealed unincorporated middle layers. This prompted the authors to use a perforated version of the mesh in the latter part of the study (39).

Post-operative adhesion is a major cause of intestinal obstruction, and may lead to bowel strangulation, necrosis and mortality (50, 51). Intraperitoneal contact with a polypropylene mesh is associated with a higher rate of adhesions and it is believed that the macroporosity and reticular structure of polypropylene meshes encourages fibroblasts integration and adherence to visceral peritoneum (52-54). The microporous laminar structure of Polytetrafluoroethylenen(ePTFE) is thought to encourage the formation of mesothelium cells parallel to the mesh surface and thus, reduce intraperitoneal adhesions (54-57). These hypotheses were consistent with our findings that adhesions formed in 50%

Downloaded by Guangxi University for Nationalities from online.liebertpub.com at 02/17/18. For personal use only.

Tissue Engineering
Cross-linked cholecyst-derived extracellular matrix for abdominal wall repair (DOI: 10.1089/ten.TEA.2017.0379)

This paper has been peer-reviewed and accepted for publication, but has yet to undergo copyediting and proof correction. The final published version may differ from this proof.

of the rabbits implanted with polypropylene, and of these, at least 25% of the mesh surfaces were involved (Figure 3). However, intraperitoneal placement of all three biologic meshes in this study were associated with very low adhesion rates. Biologic meshes are closer to a microporous laminar structure rather than a reticular macroporous structure. To avoid adhesions on the suture lines which occured in our cases, we proposed modifying the suturing technique to reduce the amount of permanent suture material on the intraperioneal side or the use of absorbable sutures.

From the analysis done on changes to dimensions of the mesh area, we found that the changes to the mesh area width was the most reliable for distinguishing stretching or contraction of the mesh area. When we examine the changes in mesh area length, which demonstrated an increase for all mesh types, we can deduce that at least a proportion, if not all, of the increase/changes seen, were caused by growth. Therefore, based on our calculations, an expected stretch of 4% and up to 10% can be attributed to growth. Prolene® meshes were known to shrink but there was a 4% increase in the mesh area length. This would mean that growth was reduced by mesh shrinkage in the Prolene® group. Hence, it was likely that growth was above 4%. In comparison, the change in length was 10% for Surgisis® meshes, a mesh known to stretch. All of the changes here could be attributed to mesh stretching or a proportion contributed by growth. Hence, it can be concluded that growth was expected to be above 4% and under 10% after 56 days.

Mesh shrinkage has plagued the performance of synthetic meshes since their introduction. We found that the area of the polypropylene shrank by 12% and 18% at day 28 and day 56, respectively (Figure 4). It is believed that scar tissues build up around synthetic filaments. When each filaments that are close together (small pore diameter <600-800 µm), the scar tissue will bridge from one filament to another across the narrow pores, forming a large scar plate across the mesh (15, 58, 59). Macroporous light weight meshes are designed to overcome this problem (60-64) by speading the filaments further apart and thus, prevent the scar tissue from bridging the wider pores.

In a preperitoneal implantation (without defect) in dogs, heavy weight polypropylene (Marlex) meshes were found to shrink by 45% in mesh area size after 4 weeks, associated with approximately 25% shortening in both vertical and horizontal

Downloaded by Guangxi University for Nationalities from online.liebertpub.com at 02/17/18. For personal use only.

Tissue Engineering
Cross-linked cholecyst-derived extracellular matrix for abdominal wall repair (DOI: 10.1089/ten.TEA.2017.0379)

This paper has been peer-reviewed and accepted for publication, but has yet to undergo copyediting and proof correction. The final published version may differ from this proof.

directions. The biggest changes were recorded between 4 to 8 weeks (65). Intraperitoneal long term placement of the Marlex mesh resulted in up to 15.8% shrinkage in a rabbit study at one year (66). In another rabbit study comparing onlay versus sublay placement of polypropylene meshes to repair 3 cm x 3 cm pararectal defects on each side, mesh area showed an average reduction of 25.9%, 28.7% and 29.0% at 30, 60, and 90 days, respectively. The onlay method (37.5% shrinkage at 90 days) showed a statistically higher shrinkage when compared with the sublay method (23.4% shrinkage) (67). Another study using a polypropylene mesh to repair a 7cm x 5cm defect in rabbits showed a 13.8% shrinkage after 90 days (68). However, in a subcutaneous implantation study in rats, a polypropylene mesh showed only 8.8% shrinkage at 56 days (69). A clinical study of 30 patients using digital radiographic evaluation, the shrinkage of a heavy weight polypropylene (Prolene®) mesh were estimated to be 7.8% at 90 days post surgery (70).

The phenomena of mesh area stretching and its clinical relevance has been largely unexplored experimentally. In this study, stretching of the mesh area was found to affect Surgisis® meshes significantly, where there was a 5% increase in size at day 28, and this increased to 48% at day 56 (Figure 4). This can be explained by the degradation of the non-crosslinked Surgisis® meshes between day 28 and day 56. Non-cross-linked CEM was also found to degrade relatively quickly in a subcutaneous implantation rat model (41, 71). By cross-linking CEM, the degradation of the EDCxCEM mesh was manipulated to prevent untimely degradation (72), while allowing cellular infiltration and mesh remodelling to take place in a slower but predictable manner (41). This was evident by the increase in the V_v of host tissue native collagen in the EDCxCEM group between day 28 and day 56 (Figure 6g).

In this study, we elected to study the response from day 28 onwards as acute inflammatory responses would be resolved at this point. Hence, host tissue responses that were related to the presence of the meshes in the period after the acute inflammation/surgical trauma phase could be evaluated. Following implantation, the processes of inflammation, mesh degradation, cellular infiltration, collagen deposition and eventual tissue remodelling were observed. The extent of each process was determined by host factors and mesh characteristics – which has been previously reviewed by our group (73).

Downloaded by Guangxi University for Nationalities from online.liebertpub.com at 02/17/18. For personal use only.

Tissue Engineering
Cross-linked cholecyst-derived extracellular matrix for abdominal wall repair (DOI: 10.1089/ten.TEA.2017.0379)

This paper has been peer-reviewed and accepted for publication, but has yet to undergo copyediting and proof correction. The final published version may differ from this proof.

Inflammation was found to be a common feature to all meshes – whether biologic or synthetic, degradable or non-degradable. It is known that inflammation plays an essential role in wound healing provided that the process is appropriate and temporary (74-79). Prolonged inflammation can lead to tissue damage and fibrosis. If the cause of inflammation is not removed, the inflammation will become chronic, causing further damage to tissues. Similarly, if a mesh is not degradable or releases damaging non-biodegradable products, the inflammation will become chronic, promoting fibrosis around the mesh (encapsulation) and/ or a foreign body reaction (73, 77, 80-84). This will continue until the cause of the inflammation is removed.

It was generally accepted that cross-linked meshes were associated with foreign body giant cells (FBGC) which are not associated with non-cross-linked meshes (85-87). FBGCs were assumed in general, to be associated with detrimental tissue response and generally not observed with degradable biologic meshes and have been cited as a negative feature (77, 80, 86). However, two interesting observations were found in this study. Firstly, we found that FBGCs were consistently present in all mesh groups (Figure 5). In the non-degradable mesh groups (Prolene® and Peri-Guard®), FBGCs were commonly found on the tissue-mesh interface. In the degradable mesh groups (EDCxCEM and Surgisis®), however, FBGCs were often observed near the degrading mesh collagen, with small pieces of collagen observed within the giant cells. The degradation sites were observed on the mesh surface initially, but progressed to the thickness of the mesh by day 56 in both the Surgisis® and EDCxCEM groups. FBGCs were known to participate in mesh degradation, as a response to “frustrated phagocytosis” when macrophages were unable to easily phagocytose the mesh in the early phase of chronic inflammation. Our observation confirmed that they actively participate in collagen-based mesh degradation. Secondly, we found that FBGCs did not persist in the mesh areas where the implanted mesh had degraded. This would suggests that their presence in the mesh area were temporary and therefore, do not always interfere negatively with tissue remodelling. Hence, we hypothesize that FBGCs in the vicinity of degrading meshes is not a negative final consequence but rather a natural host tissue response to degradation *in vivo*. Further investigation is warranted to verify this.

Downloaded by Guangxi University for Nationalities from online.liebertpub.com at 02/17/18. For personal use only.

Tissue Engineering
Cross-linked cholecyst-derived extracellular matrix for abdominal wall repair (DOI: 10.1089/ten.TEA.2017.0379)

This paper has been peer-reviewed and accepted for publication, but has yet to undergo copyediting and proof correction. The final published version may differ from this proof.

The degraded areas showed a combination of loose immature collagen and mature denser collagen, with immature collagen being observed closer to the mesh (Figure 5). These observations indicated that remodelling continued after the mesh had been degraded. The lack of mesh area stretching/ shrinkage in the EDCxCEM group showed that the remodelled tissues was adequate to prevent hernia formation in the early period. Stretching of the Surgisis® mesh would suggest untimely degradation and inadequate remodelling of the mesh area. In contrast, shrinkage of the Prolene® mesh area signifies fibrosis due to continued foreign body reaction and disorganised remodelling of the surrounding tissue.

Neovascularisation is essential for the process of initial wound healing and mesh remodelling. Neovascularisation of biologic meshes is recognised as one of the crucial properties of biologic meshes to resists bacterial infection (88, 89). Facilitation of early blood vessel ingrowth into the three-dimensional structure of meshes allows an increased number of host inflammatory cells to infiltrate the mesh. An environment within the mesh that benefited from inflammatory pathways helps to reduce and eliminate mesh infection (90, 91). Although neovascularisation is important, the ability of meshes to tolerate the presence of infection is hypothesised to be influenced by other factors, which include biomaterial porosity, degradability and surface biochemical properties. When used in a potentially contaminated field, enhancing the meshes ability to resist increased level of enzymatic degradative activity is critical to the success of its clinical objective. One method to achieve this is by providing supplementary cross-linking to the collagen structure so that a higher concentration of degradative enzymes could be tolerated, and untimely degradation avoided. In our observation (Figure 6), we found that stereological parameters for blood vessels were related to the ability to promote tissue infiltration in the earlier phase (day 28), and the demand of degradation and inflammation in the later phase (day 56). Completion of remodelling was associated with a decrease in the volume fraction of blood vessels and an increase in host collagen. This was observed as the remodelled area becomes less cellular and structurally more organised. Therefore, angiogenesis played an important role in supporting acute injury and inflammation, subsequent removal of the mesh and host degradation products, and finally contributed to the synthesis and maintenance of the remodelled host collagen matrix.

Downloaded by Guangxi University for Nationalities from online.liebertpub.com at 02/17/18. For personal use only.

Tissue Engineering
Cross-linked cholecyst-derived extracellular matrix for abdominal wall repair (DOI: 10.1089/ten.TEA.2017.0379)

This paper has been peer-reviewed and accepted for publication, but has yet to undergo copyediting and proof correction. The final published version may differ from this proof.

4. Conclusion:

In this study, the cross-linked EDCxCEM mesh prototype was compared against three established clinical products. The overall macroscopic and stereological parameters evaluated and their changes over time are summarised in the schematic diagram (Figure 7). The EDCxCEM mesh exhibited optimal biological tissue response and degradation rate in a rabbit in vivo model. Cross-linked EDCxCEM mesh demonstrated potential as a promising biologic mesh for clinical application in abdominal wall repair.

5. Funding:

The authors gratefully acknowledge the financial support from Enterprise Ireland (Technology Development Grant). This publication has emanated from research conducted with the financial support of Science Foundation Ireland (SFI) and is co-funded under the European Regional Development Fund under Grant Number 13/RC/2073. We also acknowledge support from the Centre for Microscopy & Imaging funded by NUI Galway and PRTLI, Cycles 4 and 5, National Development Plan 2007-2013.

6. Acknowledgments:

We acknowledge the graphic design assistance of Mr. Maciej Doczyk and the editorial assistance of Mr. Keith Feerick.

7. Author Disclosure Statement:

The authors report no competing financial interests exist.

Downloaded by Guangxi University for Nationalities from online.liebertpub.com at 02/17/18. For personal use only.

Tissue Engineering
Cross-linked cholecyst-derived extracellular matrix for abdominal wall repair (DOI: 10.1089/ten.TEA.2017.0379)

This paper has been peer-reviewed and accepted for publication, but has yet to undergo copyediting and proof correction. The final published version may differ from this proof.

8. References:

1. Luijendijk, R.W., Hop, W.C., van den Tol, M.P., de Lange, D.C., Braaksma, M.M., JN, I.J., Boelhouwer, R.U., de Vries, B.C., Salu, M.K., Wereldsma, J.C., Bruijninckx, C.M., andJeekel, J. A comparison of suture repair with mesh repair for incisional hernia. N Engl J Med **343**, 392, 2000.

2. Burger, J.W.A., Luijendijk, R.W., Hop, W.C.J., Halm, J.A., Verdaasdonk, E.G.G., andJeekel, J. Long-term Follow-up of a Randomized Controlled Trial of Suture Versus Mesh Repair of Incisional Hernia. Annals of Surgery **240**, 578, 2004.

3. Paul, A., Korenkov, M., Peters, S., Kohler, L., Fischer, S., andTroidl, H. Unacceptable results of the Mayo procedure for repair of abdominal incisional hernias. Eur J Surg **164**, 361, 1998.

4. Breuing, K., Butler, C.E., Ferzoco, S., Franz, M., Hultman, C.S., Kilbridge, J.F., Rosen, M., Silverman, R.P., andVargo, D. Incisional ventral hernias: review of the literature and recommendations regarding the grading and technique of repair. Surgery **148**, 544, 2010.

5. Sugerman, H.J., Kellum, J.M., Jr., Reines, H.D., DeMaria, E.J., Newsome, H.H., andLowry, J.W. Greater risk of incisional hernia with morbidly obese than steroid-dependent patients and low recurrence with prefascial polypropylene mesh. Am J Surg **171**, 80, 1996.

6. Klinge, U., Klosterhalfen, B., Muller, M., andSchumpelick, V. Foreign body reaction to meshes used for the repair of abdominal wall hernias. Eur J Surg **165**, 665, 1999.

7. Klosterhalfen, B., Klinge, U., andSchumpelick, V. Functional and morphological evaluation of different polypropylene-mesh modifications for abdominal wall repair. Biomaterials **19**, 2235, 1998.

8. Harrell, A.G., Novitsky, Y.W., Peindl, R.D., Cobb, W.S., Austin, C.E., Cristiano, J.A., Norton, J.H., Kercher, K.W., andHeniford, B.T. Prospective evaluation of adhesion formation and shrinkage of intra-abdominal prosthetics in a rabbit model. Am Surg **72**, 808, 2006.

9. Welty, G., Klinge, U., Klosterhalfen, B., Kasperk, R., andSchumpelick, V. Functional impairment and complaints following incisional hernia repair with different polypropylene meshes. Hernia **5**, 142, 2001.

10. Schumpelick, V., Arlt, G., Schlachetzki, A., andKlosterhalfen, B. [Chronic inguinal pain

Downloaded by Guangxi University for Nationalities from online.liebertpub.com at 02/17/18. For personal use only.

Tissue Engineering
Cross-linked cholecyst-derived extracellular matrix for abdominal wall repair (DOI: 10.1089/ten.TEA.2017.0379)

This paper has been peer-reviewed and accepted for publication, but has yet to undergo copyediting and proof correction. The final published version may differ from this proof.

after transperitoneal mesh implantation. Case report of net shrinkage]. Chirurg **68**, 1297, 1997.

11. McCormack, K., Scott, N., Go Peter, M.N.Y.H., Ross Sue, J., Grant, A., andCollaboration the, E.U.H.T. Laparoscopic techniques versus open techniques for inguinal hernia repair. Cochrane Database of Systematic Reviews. Chichester, UK: John Wiley & Sons, Ltd; 2003.

12. Junge, K., Klinge, U., Rosch, R., Klosterhalfen, B., andSchumpelick, V. Functional and morphologic properties of a modified mesh for inguinal hernia repair. World J Surg **26**, 1472, 2002.

13. Klosterhalfen, B., Klinge, U., Hermanns, B., andSchumpelick, V. [Pathology of traditional surgical nets for hernia repair after long-term implantation in humans]. Chirurg **71**, 43, 2000.

14. Weyhe, D., Belyaev, O., Muller, C., Meurer, K., Bauer, K.H., Papapostolou, G., andUhl, W. Improving outcomes in hernia repair by the use of light meshes--a comparison of different implant constructions based on a critical appraisal of the literature. World J Surg **31**, 234, 2007.

15. Klinge, U., Klosterhalfen, B., Birkenhauer, V., Junge, K., Conze, J., andSchumpelick, V. Impact of polymer pore size on the interface scar formation in a rat model. J Surg Res **103**, 208, 2002.

16. Bellon, J.M., Rodriguez, M., Garcia-Honduvilla, N., Gomez-Gil, V., Pascual, G., andBujan, J. Comparing the behavior of different polypropylene meshes (heavy and lightweight) in an experimental model of ventral hernia repair. J Biomed Mater Res B Appl Biomater **89**, 448, 2009.

17. Li, J., Ji, Z., andCheng, T. Lightweight versus heavyweight in inguinal hernia repair: a meta-analysis. Hernia **16**, 529, 2012.

18. O'Dwyer, P.J., Kingsnorth, A.N., Molloy, R.G., Small, P.K., Lammers, B., andHoreyseck, G. Randomized clinical trial assessing impact of a lightweight or heavyweight mesh on chronic pain after inguinal hernia repair. Br J Surg **92**, 166, 2005.

19. Cobb, W.S., Kercher, K.W., andHeniford, B.T. The argument for lightweight polypropylene mesh in hernia repair. Surg Innov **12**, 63, 2005.

20. Smietanski, M., Smietanska, I.A., Modrzejewski, A., Simons, M.P., andAufenacker, T.J. Systematic review and meta-analysis on heavy and lightweight polypropylene mesh in

Downloaded by Guangxi University for Nationalities from online.liebertpub.com at 02/17/18. For personal use only.

Tissue Engineering
Cross-linked cholecyst-derived extracellular matrix for abdominal wall repair (DOI: 10.1089/ten.TEA.2017.0379)

This paper has been peer-reviewed and accepted for publication, but has yet to undergo copyediting and proof correction. The final published version may differ from this proof.

Lichtenstein inguinal hernioplasty. Hernia **16**, 519, 2012.

21. Nikkolo, C., Murruste, M., Vaasna, T., Seepter, H., Tikk, T., andLepner, U. Three-year results of randomised clinical trial comparing lightweight mesh with heavyweight mesh for inguinal hernioplasty. Hernia **16**, 555, 2012.

22. Bittner, R., Leibl, B.J., Kraft, B., andSchwarz, J. One-year results of a prospective, randomised clinical trial comparing four meshes in laparoscopic inguinal hernia repair (TAPP). Hernia **15**, 503, 2011.

23. Yazdankhah Kenary, A., Afshin, S.N., Ahmadi Amoli, H., Yagoobi Notash, A., Borjian, A., Yagoobi Notash, A., Jr., Shafaattalab, S., andShafiee, G. Randomized clinical trial comparing lightweight mesh with heavyweight mesh for primary inguinal hernia repair. Hernia **17**, 471, 2013.

24. Zafar, H., Zaidi, M., Qadir, I., andMemon, A.A. Emergency incisional hernia repair: a difficult problem waiting for a solution. Ann Surg Innov Res **6**, 1.

25. Geisler, D.J., Reilly, J.C., Vaughan, S.G., Glennon, E.J., andKondylis, P.D. Safety and outcome of use of nonabsorbable mesh for repair of fascial defects in the presence of open bowel. Dis Colon Rectum **46**, 1118, 2003.

26. El-Khadrawy, O.H., Moussa, G., Mansour, O., andHashish, M.S. Prophylactic prosthetic reinforcement of midline abdominal incisions in high-risk patients. Hernia **13**, 267, 2009.

27. Llaguna, O.H., Avgerinos, D.V., Nagda, P., Elfant, D., Leitman, I.M., andGoodman, E. Does prophylactic biologic mesh placement protect against the development of incisional hernia in high-risk patients? World J Surg **35**, 1651, 2011.

28. Kissane, N.A., andItani, K.M. A decade of ventral incisional hernia repairs with biologic acellular dermal matrix: what have we learned? Plast Reconstr Surg **130**, 194S, 2012.

29. Janis, J.E., O'Neill, A.C., Ahmad, J., Zhong, T., andHofer, S.O. Acellular dermal matrices in abdominal wall reconstruction: a systematic review of the current evidence. Plast Reconstr Surg **130**, 183S, 2012.

30. Patel, K.M., andBhanot, P. Complications of acellular dermal matrices in abdominal wall reconstruction. Plast Reconstr Surg **130**, 216S, 2012.

31. Clemens, M.W., Selber, J.C., Liu, J., Adelman, D.M., Baumann, D.P., Garvey, P.B., andButler, C.E. Bovine versus porcine acellular dermal matrix for complex abdominal wall reconstruction. Plast Reconstr Surg **131**, 71, 2013.

Downloaded by Guangxi University for Nationalities from online.liebertpub.com at 02/17/18. For personal use only.

Tissue Engineering
Cross-linked cholecyst-derived extracellular matrix for abdominal wall repair (DOI: 10.1089/ten.TEA.2017.0379)

This paper has been peer-reviewed and accepted for publication, but has yet to undergo copyediting and proof correction. The final published version may differ from this proof.

32. Kajbafzadeh, A.M., Sabetkish, S., Heidari, R., andEbadi, M. Tissue-engineered cholecyst-derived extracellular matrix: a biomaterial for in vivo autologous bladder muscular wall regeneration. Pediatric surgery international **30**, 371, 2014.

33. Smart, N.J., Marshall, M., andDaniels, I.R. Biological meshes: a review of their use in abdominal wall hernia repairs. The surgeon : journal of the Royal Colleges of Surgeons of Edinburgh and Ireland **10**, 159, 2012.

34. Beale, E.W., Hoxworth, R.E., Livingston, E.H., andTrussler, A.P. The role of biologic mesh in abdominal wall reconstruction: a systematic review of the current literature. Am J Surg **204**, 510, 2012.

35. Purnell, C.A., Souza, J.M., Park, E., andDumanian, G.A. Repair of recurrent hernia after biologic mesh failure in abdominal wall reconstruction. The American Journal of Surgery **208**, 788, 2014.

36. Jin, J., Rosen, M.J., Blatnik, J., McGee, M.F., Williams, C.P., Marks, J., andPonsky, J. Use of acellular dermal matrix for complicated ventral hernia repair: does technique affect outcomes? J Am Coll Surg **205**, 654, 2007.

37. Nahabedian, M.Y. Does AlloDerm stretch? Plast Reconstr Surg **120**, 1276, 2007.

38. Candage, R., Jones, K., Luchette, F.A., Sinacore, J.M., Vandevender, D., andReed, R.L. Use of human acellular dermal matrix for hernia repair: Friend or foe? Surgery **144**, 703, 2008.

39. Gupta, A., Zahriya, K., Mullens, P.L., Salmassi, S., andKeshishian, A. Ventral herniorrhaphy: experience with two different biosynthetic mesh materials, Surgisis and Alloderm. Hernia **10**, 419, 2006.

40. Chan, J.C.Y., Burugapalli, K., Huang, Y.-S., Kelly, J.L., andPandit, A. A clinically relevant in vivo model for the assessment of scaffold efficacy in abdominal wall reconstruction. Journal of Tissue Engineering **8**, 2041731416686532, 2016.

41. Burugapalli, K., Chan, J.C.Y., Kelly, J.L., andPandit, A.S. Efficacy of Crosslinking on Tailoring In Vivo Biodegradability of Fibro-Porous Decellularized Extracellular Matrix and Restoration of Native Tissue Structure: A Quantitative Study using Stereology Methods. Macromolecular Bioscience **14**, 244, 2014.

42. Gilbert, T.W., Sellaro, T.L., andBadylak, S.F. Decellularization of tissues and organs. Biomaterials **27**, 3675, 2006.

Downloaded by Guangxi University for Nationalities from online.liebertpub.com at 02/17/18. For personal use only.

Tissue Engineering
Cross-linked cholecyst-derived extracellular matrix for abdominal wall repair (DOI: 10.1089/ten.TEA.2017.0379)

This paper has been peer-reviewed and accepted for publication, but has yet to undergo copyediting and proof correction. The final published version may differ from this proof.

43. Hodde, J., andHiles, M. Virus safety of a porcine-derived medical device: evaluation of a viral inactivation method. Biotechnology and bioengineering **79**, 211, 2002.

44. Pruss, A., Kao, M., Kiesewetter, H., von Versen, R., andPauli, G. Virus safety of avital bone tissue transplants: evaluation of sterilization steps of spongiosa cuboids using a peracetic acid-methanol mixture. Biologicals : journal of the International Association of Biological Standardization **27**, 195, 1999.

45. Yoganarasimha, S., Trahan, W.R., Best, A.M., Bowlin, G.L., Kitten, T.O., Moon, P.C., andMadurantakam, P.A. Peracetic acid: a practical agent for sterilizing heat-labile polymeric tissue-engineering scaffolds. Tissue engineering Part C, Methods **20**, 714, 2014.

46. Kemp, P.D. Peracetic acid sterilization of collagen or collagenous tissue. Google Patents; 1995.

47. Group, S.M.S. Prophylaxis of pelvic sidewall adhesions with Gore-Tex surgical membrane: a multicenter clinical investigation. . Fertil Steril **57**, 921, 1992.

48. Garcia, Y., Breen, A., Burugapalli, K., Dockery, P., andPandit, A. Stereological methods to assess tissue response for tissue-engineered scaffolds. Biomaterials **28**, 175, 2007.

49. Bali, C., Papakostas, J., Georgiou, G., Kouvelos, G., Avgos, S., Arnaoutoglou, E., Papadopoulos, G., andMatsagkas, M. A comparative study of sutured versus bovine pericardium mesh abdominal closure after open abdominal aortic aneurysm repair. Hernia.

50. Gonzalez, R., Rodeheaver, G.T., Moody, D.L., Foresman, P.A., andRamshaw, B.J. Resistance to adhesion formation: a comparative study of treated and untreated mesh products placed in the abdominal cavity. Hernia **8**, 213, 2004.

51. Menzies, D. Postoperative adhesions: their treatment and relevance in clinical practice. Ann R Coll Surg Engl **75**, 147, 1993.

52. Bellon, J.M., Contreras, L.A., Bujan, J., andCarrera-San Martin, A. The use of biomaterials in the repair of abdominal wall defects: a comparative study between polypropylene meshes (Marlex) and a new polytetrafluoroethylene prosthesis (Dual Mesh). J Biomater Appl **12**, 121, 1997.

53. Farmer, L., Ayoub, M., Warejcka, D., Southerland, S., Freeman, A., andSolis, M. Adhesion formation after intraperitoneal and extraperitoneal implantation of polypropylene mesh. Am Surg **64**, 144, 1998.

54. Matthews, B.D., Pratt, B.L., Pollinger, H.S., Backus, C.L., Kercher, K.W., Sing, R.F.,

Downloaded by Guangxi University for Nationalities from online.liebertpub.com at 02/17/18. For personal use only.

Tissue Engineering
Cross-linked cholecyst-derived extracellular matrix for abdominal wall repair (DOI: 10.1089/ten.TEA.2017.0379)

This paper has been peer-reviewed and accepted for publication, but has yet to undergo copyediting and proof correction. The final published version may differ from this proof.

andHeniford, B.T. Assessment of adhesion formation to intra-abdominal polypropylene mesh and polytetrafluoroethylene mesh. J Surg Res **114**, 126, 2003.

55. Bellon, J.M., Garcia-Carranza, A., Jurado, F., Garcia-Honduvilla, N., Carrera-San Martin, A., andBujan, J. Peritoneal regeneration after implant of a composite prosthesis in the abdominal wall. World J Surg **25**, 147, 2001.

56. Bellon, J.M., Jurado, F., Garcia-Honduvilla, N., Lopez, R., Carrera-San Martin, A., andBujan, J. The structure of a biomaterial rather than its chemical composition modulates the repair process at the peritoneal level. Am J Surg **184**, 154, 2002.

57. Bellon, J.M., Jurado, F., Garcia-Moreno, F., Corrales, C., Carrera-San Martin, A., andBujan, J. Healing process induced by three composite prostheses in the repair of abdominal wall defects. J Biomed Mater Res **63**, 182, 2002.

58. Klosterhalfen, B., Junge, K., andKlinge, U. The lightweight and large porous mesh concept for hernia repair. Expert Rev Med Devices **2**, 103, 2005.

59. Klinge, U., Klosterhalfen, B., Muller, M., Anurov, M., Ottinger, A., andSchumpelick, V. Influence of polyglactin-coating on functional and morphological parameters of polypropylene-mesh modifications for abdominal wall repair. Biomaterials **20**, 613, 1999.

60. Klinge, U., Klosterhalfen, B., Conze, J., Limberg, W., Obolenski, B., Ottinger, A.P., andSchumpelick, V. Modified mesh for hernia repair that is adapted to the physiology of the abdominal wall. Eur J Surg **164**, 951, 1998.

61. Cobb, W.S., Burns, J.M., Peindl, R.D., Carbonell, A.M., Matthews, B.D., Kercher, K.W., andHeniford, B.T. Textile analysis of heavy weight, mid-weight, and light weight polypropylene mesh in a porcine ventral hernia model. J Surg Res **136**, 1, 2006.

62. Schmidbauer, S., Ladurner, R., Hallfeldt, K.K., andMussack, T. Heavy-weight versus low-weight polypropylene meshes for open sublay mesh repair of incisional hernia. Eur J Med Res **10**, 247, 2005.

63. Berrevoet, F., Maes, L., De Baerdemaeker, L., Rogiers, X., Troisi, R., andde Hemptinne, B. Comparable results with 3-year follow-up for large-pore versus small-pore meshes in open incisional hernia repair. Surgery **148**, 969.

64. Klinge, U., andKlosterhalfen, B. Modified classification of surgical meshes for hernia repair based on the analyses of 1,000 explanted meshes. Hernia **16**, 251, 2012.

65. Klinge, U., Klosterhalfen, B., Muller, M., Ottinger, A.P., andSchumpelick, V. Shrinking of

Downloaded by Guangxi University for Nationalities from online.liebertpub.com at 02/17/18. For personal use only.

Tissue Engineering
Cross-linked cholecyst-derived extracellular matrix for abdominal wall repair (DOI: 10.1089/ten.TEA.2017.0379)

This paper has been peer-reviewed and accepted for publication, but has yet to undergo copyediting and proof correction. The final published version may differ from this proof.

polypropylene mesh in vivo: an experimental study in dogs. Eur J Surg **164**, 965, 1998.

66. Novitsky, Y.W., Harrell, A.G., Cristiano, J.A., Paton, B.L., Norton, H.J., Peindl, R.D., Kercher, K.W., andHeniford, B.T. Comparative evaluation of adhesion formation, strength of ingrowth, and textile properties of prosthetic meshes after long-term intra-abdominal implantation in a rabbit. J Surg Res **140**, 6, 2007.

67. Garcia-Urena, M.A., Vega Ruiz, V., Diaz Godoy, A., Baez Perea, J.M., Marin Gomez, L.M., Carnero Hernandez, F.J., andVelasco Garcia, M.A. Differences in polypropylene shrinkage depending on mesh position in an experimental study. Am J Surg **193**, 538, 2007.

68. Bellon, J.M., Garcia-Honduvilla, N., Rodriguez, M., Pascual, G., Gomez-Gil, V., andBujan, J. Influence of the structure of new generation prostheses on shrinkage after implant in the abdominal wall. J Biomed Mater Res B Appl Biomater **78**, 340, 2006.

69. Junge, K., Rosch, R., Krones, C.J., Klinge, U., Mertens, P.R., Lynen, P., Schumpelick, V., andKlosterhalfen, B. Influence of polyglecaprone 25 (Monocryl) supplementation on the biocompatibility of a polypropylene mesh for hernia repair. Hernia **9**, 212, 2005.

70. Silvestre, A.C., de Mathia, G.B., Fagundes, D.J., Medeiros, L.R., andRosa, M.I. Shrinkage evaluation of heavyweight and lightweight polypropylene meshes in inguinal hernia repair: a randomized controlled trial. Hernia **15**, 629, 2011.

71. Burugapalli, K., andPandit, A. Characterization of tissue response and in vivo degradation of cholecyst-derived extracellular matrix. Biomacromolecules **8**, 3439, 2007.

72. Burugapalli, K., Chan, J.C., Naik, H., Kelly, J.L., andPandit, A. Tailoring the properties of cholecyst-derived extracellular matrix using carbodiimide cross-linking. Journal of biomaterials science Polymer edition **20**, 1049, 2009.

73. Chan, J.C.Y., Burugapalli, K., Kelly, J.L., Pandit, A. Influence of Clinical Application on Bioresorbability: Host Response. In: Buchanan F., ed. Degradation Rate of Bioresorbable Materials: Prediction and Evaluation. Cambridge, England: Woodhead Publishing Ltd.; 2008. pp. 267.

74. Jean-Baptiste, E. Cellular mechanisms in sepsis. J Intensive Care Med **22**, 63, 2007.

75. Raghow, R. The role of extracellular matrix in postinflammatory wound healing and fibrosis. FASEB J **8**, 823, 1994.

76. Park, J.E., andBarbul, A. Understanding the role of immune regulation in wound healing. Am J Surg **187**, 11S, 2004.

77. Anderson, J.M. Biological responses to materials. Annual Review of Materials Research **31**, 81, 2001.

78. Bogdan, C., andNathan, C. Modulation of macrophage function by transforming growth factor beta, interleukin-4, and interleukin-10. Ann N Y Acad Sci **685**, 713, 1993.

79. Franz, S., Rammelt, S., Scharnweber, D., andSimon, J.C. Immune responses to implants - a review of the implications for the design of immunomodulatory biomaterials. Biomaterials **32**, 6692, 2011.

80. Anderson, J.M., Defife, K., McNally, A., Collier, T., andJenney, C. Monocyte, macrophage and foreign body giant cell interactions with molecularly engineered surfaces. J Mater Sci Mater Med **10**, 579, 1999.

81. Liang, H.C., Chang, Y., Hsu, C.K., Lee, M.H., andSung, H.W. Effects of crosslinking degree of an acellular biological tissue on its tissue regeneration pattern. Biomaterials **25**, 3541, 2004.

82. Hunt, J.A., Remes, A., andWilliams, D.F. Stimulation of neutrophil movement by metal ions. J Biomed Mater Res **26**, 819, 1992.

83. Hunt, J.A., Flanagan, B.F., McLaughlin, P.J., Strickland, I., andWilliams, D.F. Effect of biomaterial surface charge on the inflammatory response: evaluation of cellular infiltration and TNF alpha production. J Biomed Mater Res **31**, 139, 1996.

84. Hamilton, J.A. Nondisposable materials, chronic inflammation, and adjuvant action. J Leukoc Biol **73**, 702, 2003.

85. Badylak, S.F. Xenogeneic extracellular matrix as a scaffold for tissue reconstruction. Transpl Immunol **12**, 367, 2004.

86. Novitsky, Y.W., Orenstein, S.B., andKreutzer, D.L. Comparative analysis of histopathologic responses to implanted porcine biologic meshes. Hernia 2013.

87. Badylak, S.F., Freytes, D.O., andGilbert, T.W. Extracellular matrix as a biological scaffold material: Structure and function. Acta Biomater **5**, 1, 2009.

88. Rice, R.D., Ayubi, F.S., Shaub, Z.J., Parker, D.M., Armstrong, P.J., andTsai, J.W. Comparison of Surgisis, AlloDerm, and Vicryl Woven Mesh grafts for abdominal wall defect repair in an animal model. Aesthetic Plast Surg **34**, 290, 2010.

89. Menon, N.G., Rodriguez, E.D., Byrnes, C.K., Girotto, J.A., Goldberg, N.H., andSilverman, R.P. Revascularization of human acellular dermis in full-thickness abdominal wall reconstruction in the rabbit model. Ann Plast Surg **50**, 523, 2003.

Downloaded by Guangxi University for Nationalities from online.liebertpub.com at 02/17/18. For personal use only.

Tissue Engineering
Cross-linked cholecyst-derived extracellular matrix for abdominal wall repair (DOI: 10.1089/ten.TEA.2017.0379)

This paper has been peer-reviewed and accepted for publication, but has yet to undergo copyediting and proof correction. The final published version may differ from this proof.

90. Franklin, M.E., Jr., Trevino, J.M., Portillo, G., Vela, I., Glass, J.L., andGonzalez, J.J. The use of porcine small intestinal submucosa as a prosthetic material for laparoscopic hernia repair in infected and potentially contaminated fields: long-term follow-up. Surg Endosc **22**, 1941, 2008.

91. Patton, J.H., Jr., Berry, S., andKralovich, K.A. Use of human acellular dermal matrix in complex and contaminated abdominal wall reconstructions. Am J Surg **193**, 360, 2007.

Downloaded by Guangxi University for Nationalities from online.liebertpub.com at 02/17/18. For personal use only.

Tissue Engineering
Cross-linked cholecyst-derived extracellular matrix for abdominal wall repair (DOI: 10.1089/ten.TEA.2017.0379)

This paper has been peer-reviewed and accepted for publication, but has yet to undergo copyediting and proof correction. The final published version may differ from this proof.

Figure Legends

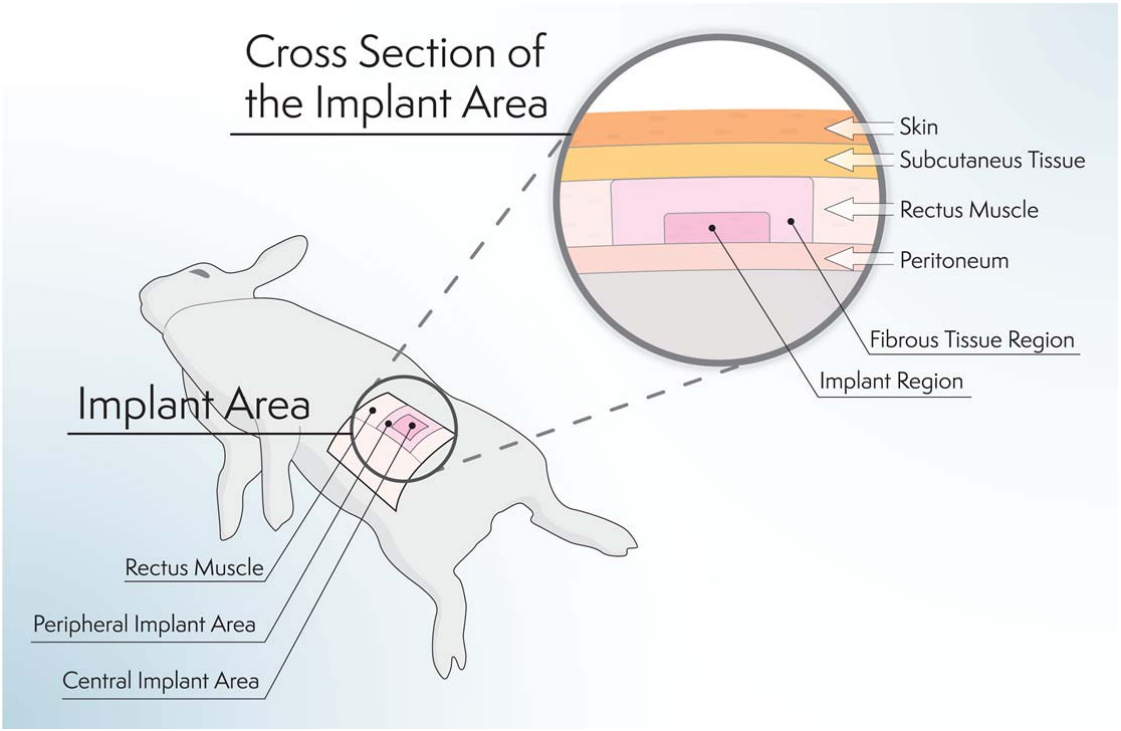

Figure 1: Schematic diagram showing a cross section of the implant area with the implant region, and fibrous tissue region, showing the central implant area (CA) and peripheral implant area.

Downloaded by Guangxi University for Nationalities from online.lieberpub.com at 02/17/18. For personal use only.

Tissue Engineering
Cross-linked cholecyst-derived extracellular matrix for abdominal wall repair (DOI: 10.1089/ten.TEA.2017.0379)

This paper has been peer-reviewed and accepted for publication, but has yet to undergo copyediting and proof correction. The final published version may differ from this proof.

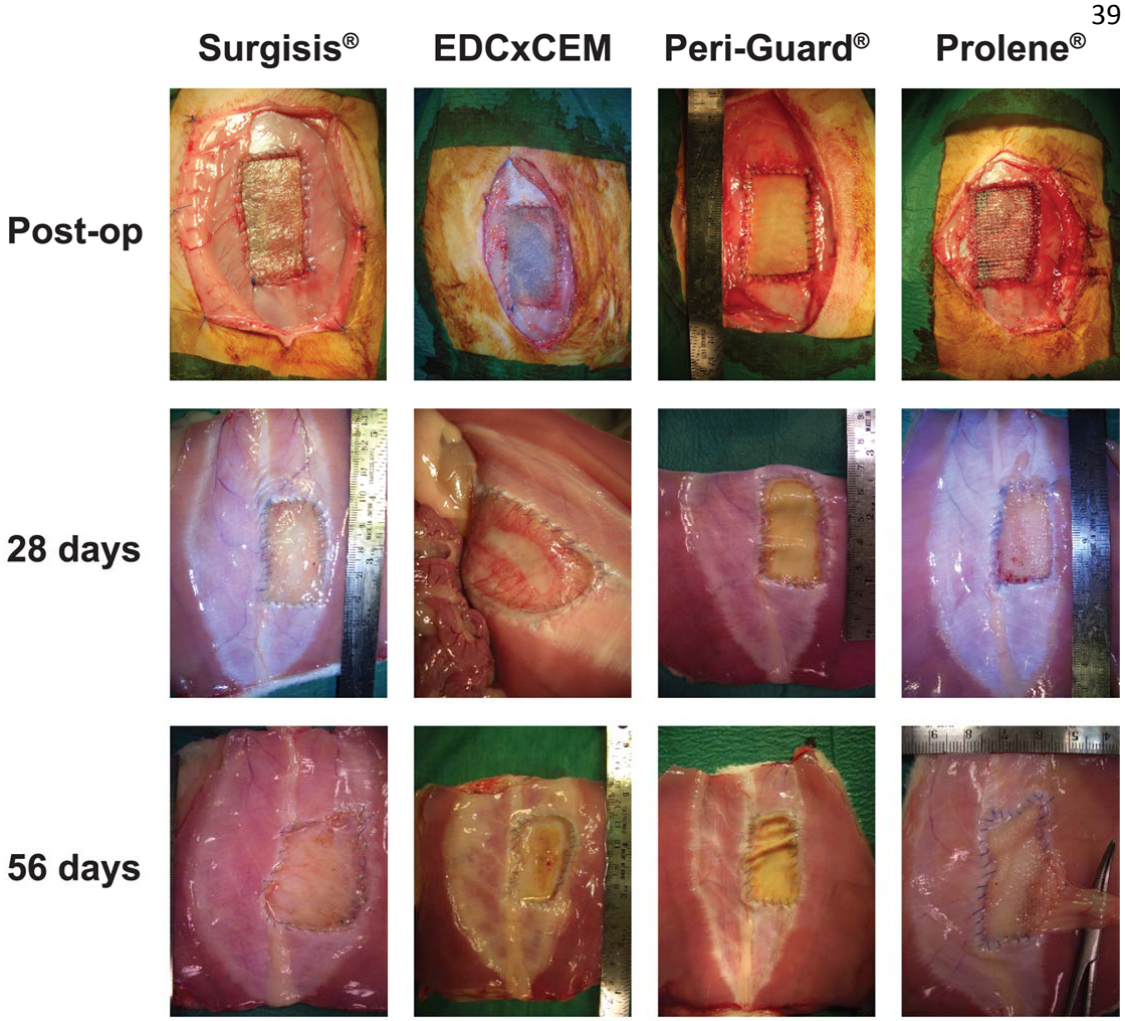

Figure 2: Macroscopic appearance of the meshed meshes after abdominal wall repair surgery immediately (post-op), 28 days, and 56 days.

Downloaded by Guangxi University for Nationalities from online.liebertpub.com at 02/17/18. For personal use only.

Tissue Engineering
Cross-linked cholecyst-derived extracellular matrix for abdominal wall repair (DOI: 10.1089/ten.TEA.2017.0379)

This paper has been peer-reviewed and accepted for publication, but has yet to undergo copyediting and proof correction. The final published version may differ from this proof.

Downloaded by Guangxi University for Nationalities from online.liebertpub.com at 02/17/18. For personal use only.

Tissue Engineering
Cross-linked cholecyst-derived extracellular matrix for abdominal wall repair (DOI: 10.1089/ten.TEA.2017.0379)

This paper has been peer-reviewed and accepted for publication, but has yet to undergo copyediting and proof correction. The final published version may differ from this proof.

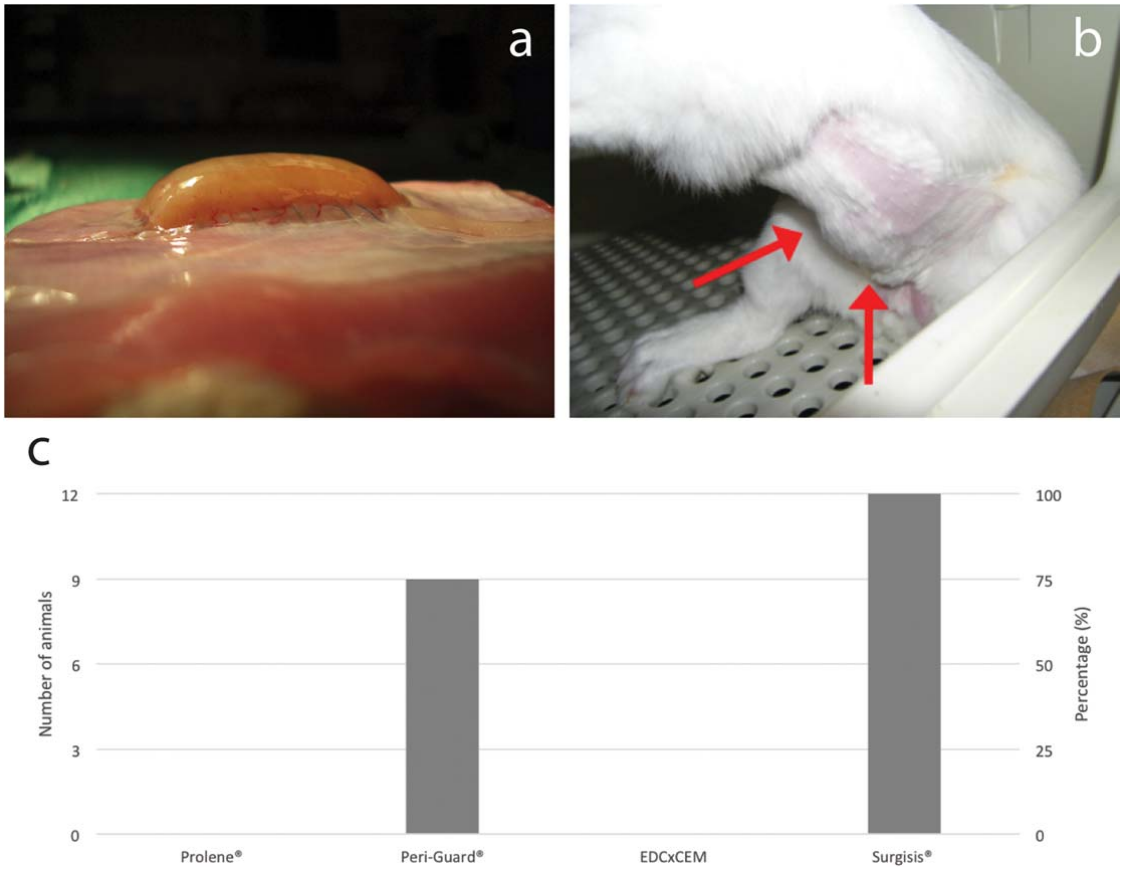

Figure 3: Seroma formation *in vivo*: (a) photograph of seroma fluid within the layers of the Surgisis® mesh (b) seroma visible on abdominal wall after Surgisis® mesh implantation, (c) numbers of seroma formed for the meshes. No seroma formation was observed for Prolene® and EDCxCEM meshes.

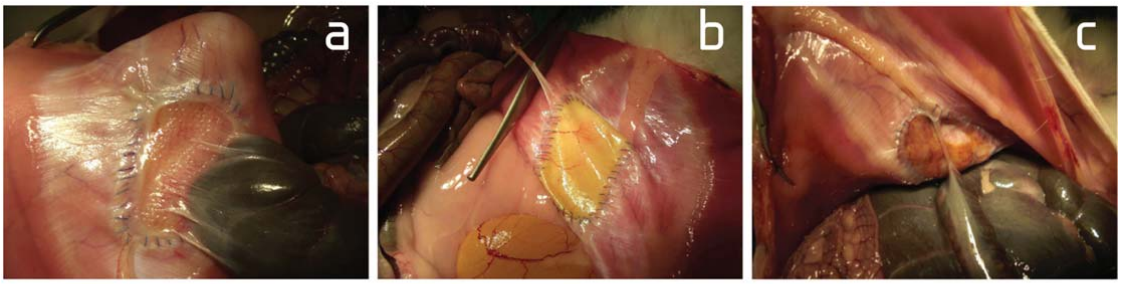

d

Implants	Time	Number of cases	Adhesion scores for each case			Adhesion score Mean (SD)
			Extent/ Area (0-4)	Type (0-4)	Tenacity (0-3)	
Prolene®	28 days	3/6	3, 2, 2	2, 3, 2	3, 3, 3	3.8 (4.2)
	56 days	3/6	3, 2, 2	2, 2, 4	3, 3, 3	4 (4.4)
Peri-Guard®	28 days	0/6				
	56 days	2/6	1, 1	1, 2	3, 3	1.8 (2.9)
EDCxCEM	28 days	0/6				
	56 days	1/6	1	2	3	1 (2.4)
Surgisis®	28 days	0/6				
	56 days	0/6				

Figure 4: Intraabdominal adhesions in (a) Prolene®, (b) Peri-Guard®, and (c) EDCxCEM meshes. (d) Analysis of adhesion using the scoring method developed by the Surgical Membrane Study Group (1992). No statistical significance among groups (ANOVA, $p>0.05$ between all pairs) was observed.

Downloaded by Guangxi University for Nationalities from online.liebertpub.com at 02/17/18. For personal use only.

Tissue Engineering
Cross-linked cholecyst-derived extracellular matrix for abdominal wall repair (DOI: 10.1089/ten.TEA.2017.0379)

This paper has been peer-reviewed and accepted for publication, but has yet to undergo copyediting and proof correction. The final published version may differ from this proof.

Downloaded by Guangxi University for Nationalities from online.liebertpub.com at 02/17/18. For personal use only.

Tissue Engineering
Cross-linked cholecyst-derived extracellular matrix for abdominal wall repair (DOI: 10.1089/ten.TEA.2017.0379)

This paper has been peer-reviewed and accepted for publication, but has yet to undergo copyediting and proof correction. The final published version may differ from this proof.

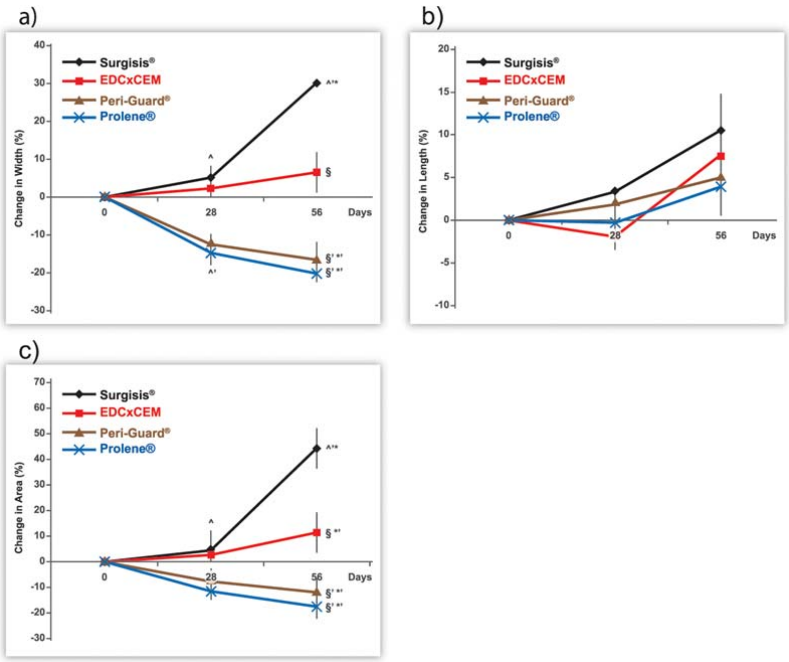

Figure 5: Percentage change in (a) width, (b) length, and (c) mesh area following implantation at 28 and 56 days.

Downloaded by Guangxi University for Nationalities from online.liebertpub.com at 02/17/18. For personal use only.

Tissue Engineering
Cross-linked cholecyst-derived extracellular matrix for abdominal wall repair (DOI: 10.1089/ten.TEA.2017.0379)

This paper has been peer-reviewed and accepted for publication, but has yet to undergo copyediting and proof correction. The final published version may differ from this proof.

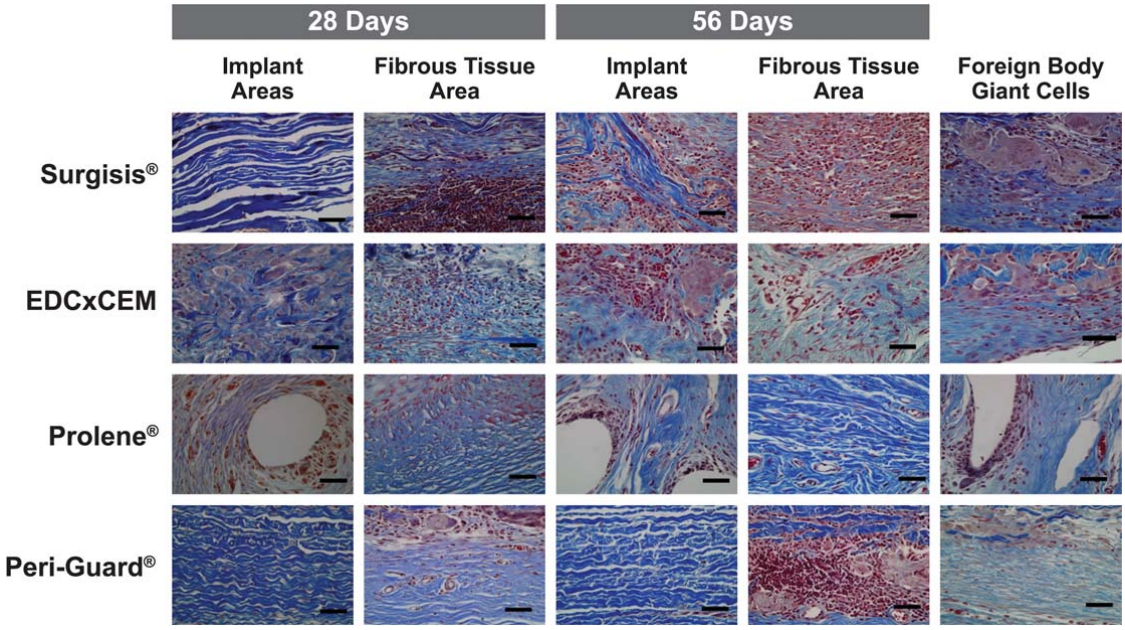

Figure 6: Masson's Trichrome stained histology sections showing mesh area and fibrous tissue area, and foreign body giant cells in the tested groups. (Bar 50µm).

Downloaded by Guangxi University for Nationalities from online.liebertpub.com at 02/17/18. For personal use only.

Tissue Engineering
Cross-linked cholecyst-derived extracellular matrix for abdominal wall repair (DOI: 10.1089/ten.TEA.2017.0379)

This paper has been peer-reviewed and accepted for publication, but has yet to undergo copyediting and proof correction. The final published version may differ from this proof.

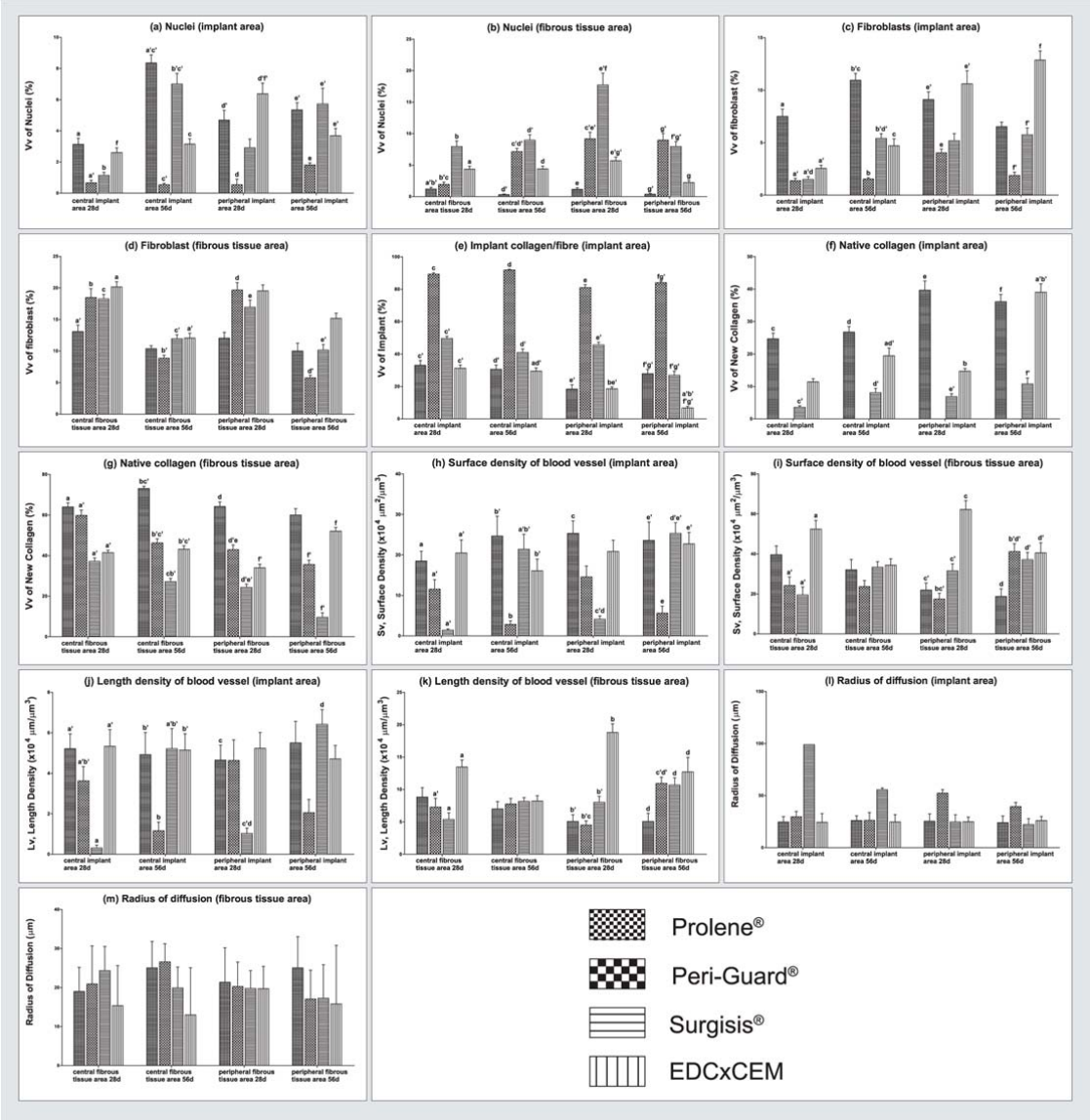

Figure 7: Quantification of stereological analysis in volume fraction of (a,b) nuclei, (c,d) fibroblasts, (e) mesh, (f,g) collagen; (h,i) surface/ (j,k) length density of blood vessel, and (l,m) radius of diffusion; X-axis legend (left to right) on (a-m); central implant area 28d; central implant area 56d; peripheral implant area 28d; peripheral area 56d.

Downloaded by Guangxi University for Nationalities from online.liebertpub.com at 02/17/18. For personal use only.

Tissue Engineering
Cross-linked cholecyst-derived extracellular matrix for abdominal wall repair (DOI: 10.1089/ten.TEA.2017.0379)

This paper has been peer-reviewed and accepted for publication, but has yet to undergo copyediting and proof correction. The final published version may differ from this proof.

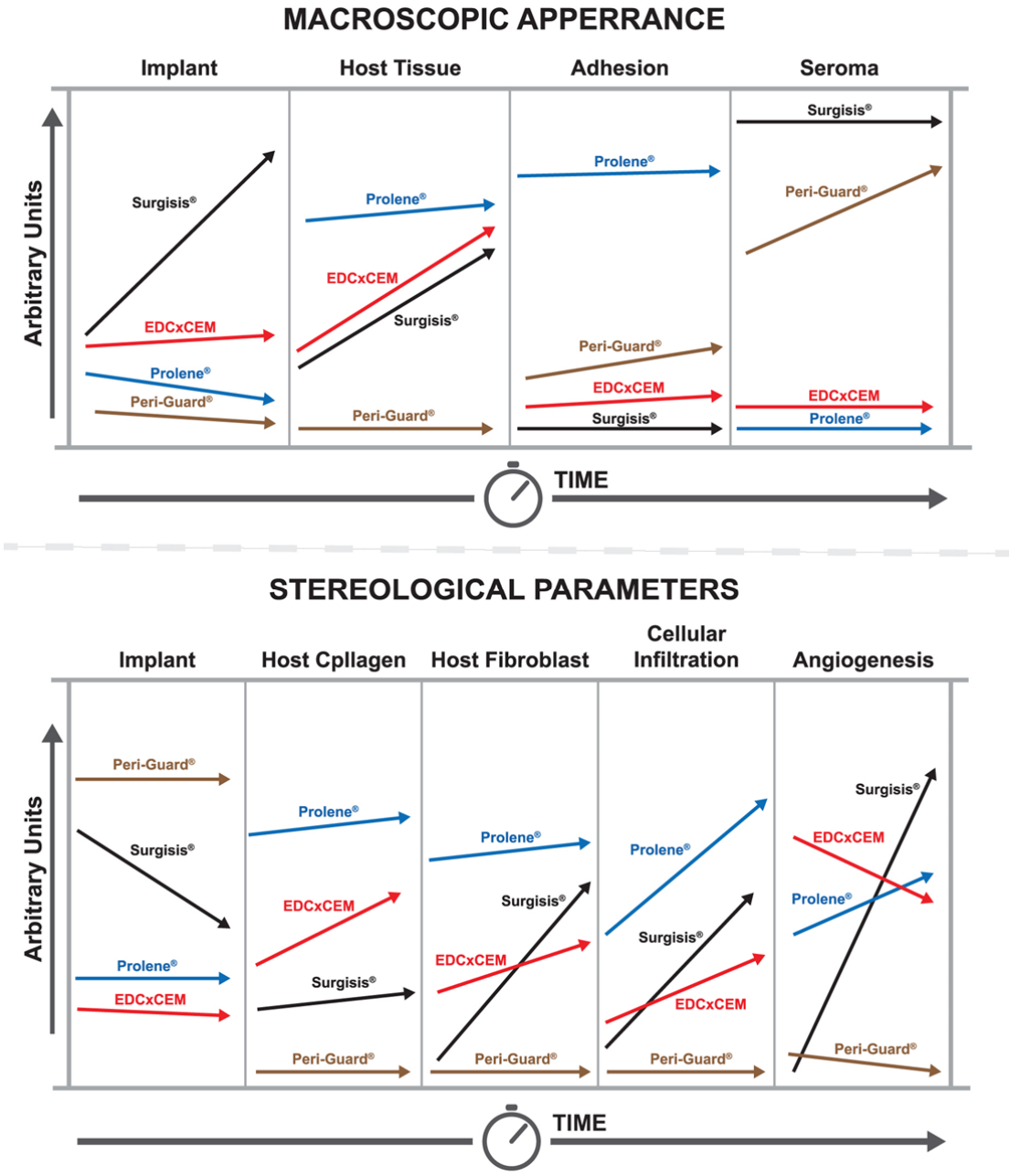

Figure 8: Summary of macroscopic appearance (top) and stereological parameters (bottom) of four meshes investigated in this study.